Fig. 5. Immunostaining with anti-GAD65 antibody in the hippocampus of control, hypothyroid and T4-replacement groups at PND28.

Hippocampal sections (8 μm thick) from control, hypothyroid and T4-replacement groups at PND28 were stained with anti-GAD65 antibody. (A) Representataive photomicrographs of the hippocampal subregions (CA1, CA3 and DG) of control, hypothyroid and T4-replacement groups at PND28. These sections were adjacent to the sections shown in Fig. 4. (B) The number of GAD65-positive cells in the whole hippocampus and the hippocampal subregions (CA1, CA2, CA3 and DG) of control (open bar), hypothyroid (solid bar) and T4-replacement groups (shaded bar) were counted in each section obtained at PND28 and expressed as means + SEM. $n = 5$–6 (control, hypothyroid, T4-replacement groups). o: stratum oriens, py: stratum pyramidale, r: stratum radiatum, luc: stratum lucidum, m: stratum moleculare, g: stratum granulare, h: hilus. $*P < 0.05$ between control and hypothyroid groups. $^\#P < 0.05$ between hypothyroid and T4-replacement groups.

4. Discussion

4.1. Sensitivity of the hippocampus toward TH status during development

By comparing the expression profiles of three TH-dependent genes in the three experimental groups, we confirmed that the developing hippocampus was one of the highly TH-sensitive brain regions (Fig. 2). Hippocampal neurons exhibit high expression levels of both TH receptors (Bradley et al., 1992) and the monocarboxylate transporter 8 (MCT8; slc16a2) (Heuer et al., 2005) identified as a specific TH transporter in the brain (Friesema et al., 2003). In addition, type 2 deiodinase responsible for converting T4 into active T3 is highly expressed in astrocytes in the hippocampus, especially in the dentate gyrus (Guadaño-Ferraz et al., 1997). High sensitivity of the hippocampus toward TH thus results from the abundant expression of its receptors as well as molecules regulating T3 availability in this region during the perinatal period.
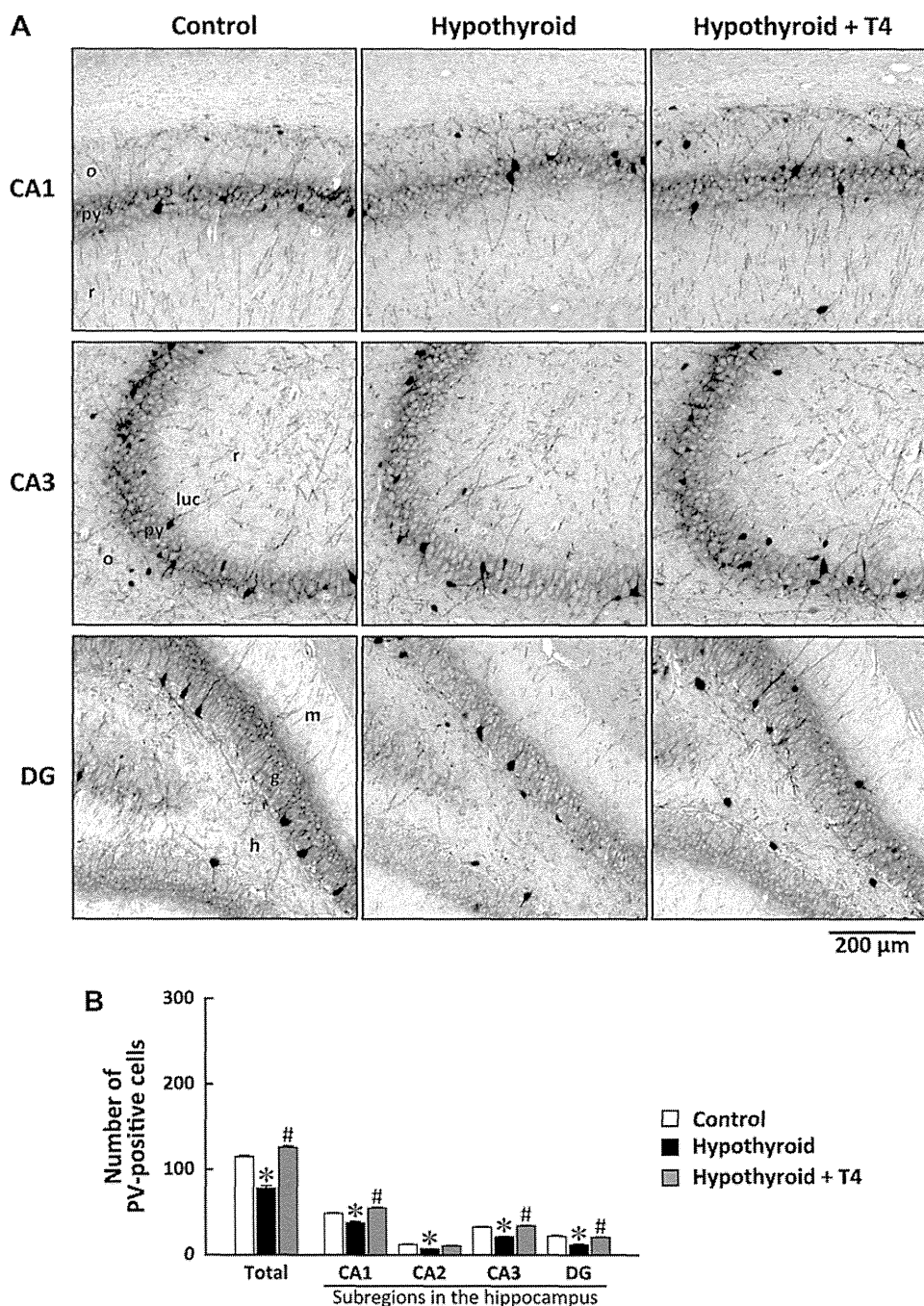
Fig. 6. Immunostaining with anti-PV antibody in the hippocampus of control, hypothyroid and T4-replacement groups at PND28. Hippocampal sections (8 μm thick) from control, hypothyroid and T4-replacement groups at PND28 were stained with anti-PV antibody. (A) Representataive photomicrographs of the hippocampal subregions (CA1, CA3 and DG) of control, hypothyroid and T4-replacement groups at PND28. These sections were adjacent to the sections shown in Fig. 4. (B) The number of PV-positive cells in the whole hippocampus and the hippocampal subregions (CA1, CA2, CA3 and DG) of control (open bar), hypothyroid (solid bar) and T4-replacement groups (shaded bar) were counted in each section obtained at PND28 and expressed as means + SEM. $n = 5$–6 (control, hypothyroid, T4-replacement groups). o: stratum oriens, py: stratum pyramidale, r: stratum radiatum, luc: stratum lucidum, m: stratum moleculare, g: stratum granulare, h: hilus. *$P < 0.05$ between control and hypothyroid groups. #$P < 0.05$ between hypothyroid and T4-replacement groups.

4.2. TH affects the phenotype of GABAergic neurons in the developing hippocampus

In the present study, the two GAD isotypes, GAD67 and GAD65, were shown to be differentially affected by hypothyroidism. Reduction of GAD65 protein to 50% or less of the control level was observed at PND4, 15 and 28 (Fig. 3B) which was correlated immunohistochemically with a 37% reduction of GAD65-positive cells as well as reduction of GAD65-positive processes and terminals at PND28 (Fig. 5). In contrast, the amount of GAD67 protein or the number of GAD67-positive cells was not affected by hypothyroidism (Figs. 3A and 4). The two isotypes originating from two distinct genes differ in their intracellular distribution and regulation. GAD67 exists as an active form with bound coenzyme and is localized throughout the cytosol of GABAergic neurons, whereas GAD65 is predominantly in an inactive form without the coenzyme and is enriched in nerve terminals (Erlander et al., 1991; Esclapez et al., 1994; Fukuda et al., 1997). In the rodent
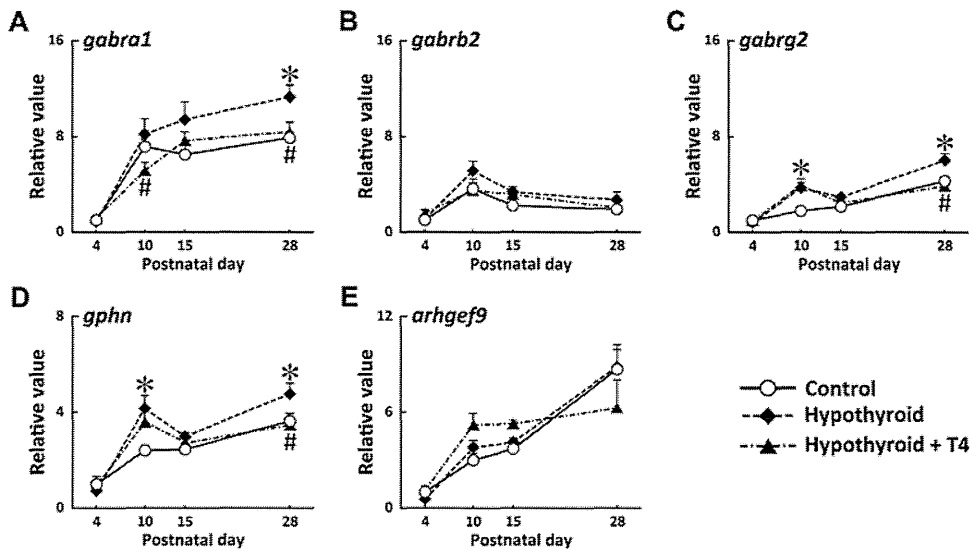
Fig. 7. Comparison of expression profiles of the inhibitory post-synaptic component genes in the hippocampus of control, hypothyroid and T4-replacement groups during development. The mRNA expression of GABA(A) receptor subunits (A: gabra1, B: gabrb2, C: gabrg2) and the inhibitory scaffolding protein (D: gphn, E: arhgef9) in the hippocampus of pups in the control (open circles), hypothyroid (solid squares) and T4-replacement groups (solid triangles) was quantified by real-time PCR at PND4, 10, 15 and 28 using ppia as internal standard. Each mRNA level is expressed relative to that of the control group at PND4 (means + SEM of 5 rats/group/age). $^{*}P < 0.05$ between control and hypothyroid groups. $^{\#}P < 0.05$ between hypothyroid and T4-replacement groups.
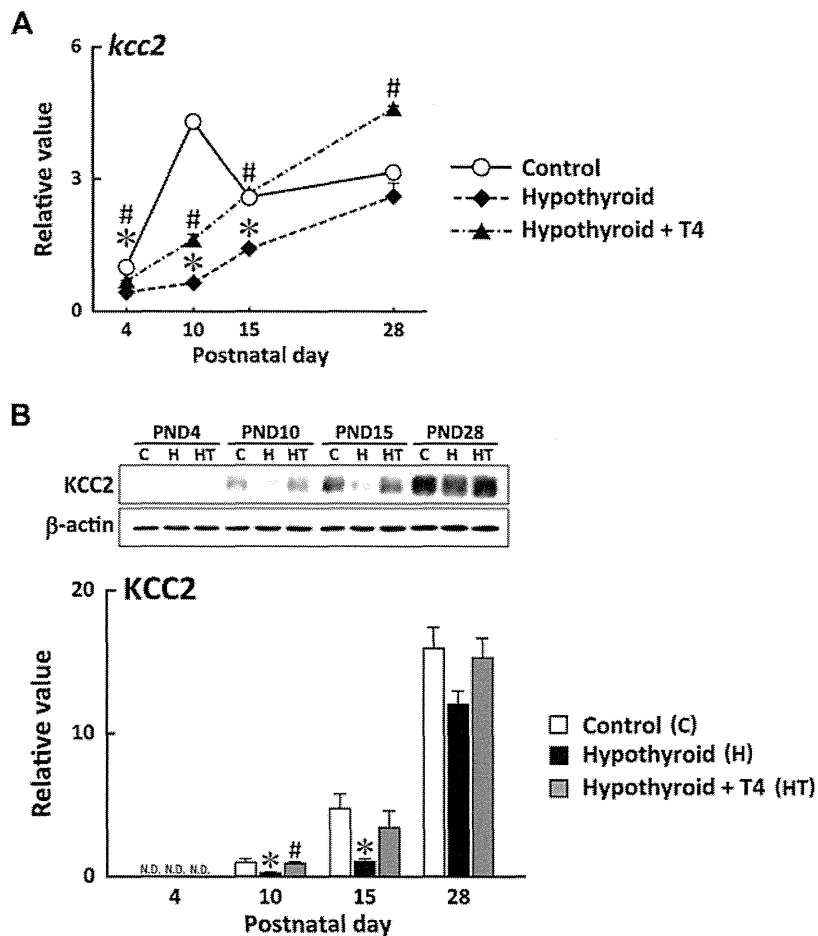

Fig. 8. Comparison of mRNA and protein expressions of kcc2 gene in the hippocampus of control, hypothyroid and T4-replacement groups during development. (A) The mRNA expression of kcc2 in the hippocampus of control (open circles), hypothyroid (solid squares) and T4-replacement groups (solid triangles) were quantified by real-time PCR at PND4, 10, 15 and 28 using ppia as internal standard. Each mRNA level is expressed relative to that of the control group at PND4 (means + SEM of 5 rats/group/age). (B) KCC2 protein level quantified by Western blotting with anti-KCC2 antibody. Immunoreactive band of KCC2 (examples shown in upper panels) in the hippocampus of control (open bar), hypothyroid (solid bar), T4-replacement groups (shaded bar) at PND4, 10, 15 and 28 were quantified using β-actin as standard and expressed relative to that of the control group at PND10 (means + SEM of 5 rats/group/age). N.D.: not detected. $^{*}P < 0.05$ between control and hypothyroid groups. $^{\#}P < 0.05$ between hypothyroid and T4-replacement groups.

hippocampus, most GABAergic neurons exhibit moderate to intense GAD67 immunoreactivity in somata, but some of them show markedly low immunoreactivity toward GAD65 (Fukuda et al., 1997). Furthermore, GABAergic terminals located in the perisomatic domain of principal neurons show intense immunoreactivity toward GAD67 whereas those in the dendritic domain show stronger immunoreactivity toward GAD65 (Fukuda et al., 1998). Our results thus show that the total number of GABAergic neurons was not affected by TH status but the expression of GAD65 both in somata and processes was TH-dependent.

Parvalbumin (PV) is an intracellular Ca^{2+} buffering protein which is considered as a marker for a subpopulation of hippocampal GABAergic neurons (Chard et al., 1993; Fukuda et al., 1997). PV-positive cells and their processes were dramatically reduced in the hypothyroid hippocampus (Fig. 6) as reported previously in models of hypothyroidism induced chemically with PTU or MMI as well as in TRα knockout mice and mice possessing mutated TRα with low affinity toward T3 (Gilbert et al., 2007; Guadaño-Ferraz et al., 2003; Venero et al., 2005). PV-positive cells are mainly located in the pyramidal cell layer and contribute to fast- spiking, perisomatic input onto pyramidal cells (Fukuda et al., 1997). In a previous study on animals developmentally exposed to lower doses of PTU, no change in GAD67-immunoreactivity was detected while PV-positive cells were reduced in number (Gilbert et al., 2007).

The results of the present study thus confirm that the total number of GABAergic neurons in the hippocampus was not affected but the phenotype of GABAergic neurons was significantly altered and GABAergic processes and terminals were reduced by developmental hypothyroidism. Such alterations lead to impairments in circuit formation and inhibitory function in the hippocampus as detected by electrophysiological methods (Guadaño-Ferraz et al., 2003; Gilbert et al., 2007).

4.3. TH-dependent expression of KCC2 and maturation of the GABAergic system

The postsynaptic components of the GABAergic system including GABA(A) receptor subunits (α1, γ2) and gephyrin (a scaffold protein localized to inhibitory synapses) showed TH-responsive expression changes (up-regulated in hypothyroid and normalized by T4-replacement) only at a later stage of PND28 (Fig. 7), possibly reflecting a decrease in GABA release in the hypothyroid state.

In contrast, expression of the neuron-specific K^+/Cl^- co-transporter, kcc2, was positively regulated by TH from PND4, prior to increases in mRNA expression of GABARs (Fig. 8). A sharp rise of kcc2 mRNA expression observed at PND10 in the control animal was TH-dependent and resulted in a 4.8-fold increase in KCC2 protein between PND10 and 15, which corresponds to the switching of GABA action from excitatory to inhibitory (Payne et al., 2003; Ben-Ari et al., 2007; Farrant and Kaila, 2007). Absence of this rise in kcc2 expression led to a marked reduction in KCC2 protein at PND15 (Fig. 8B), suggesting a significant delay in the excitatory to inhibitory switching of GABA action as detected electrophysiologically in hippocampal slices from hypothyroid animals by Friauf et al. (2008b). In contrast to our observation, these authors detected no difference in the intensity or localization of KCC2 immunoreactivity in the auditory brain stem of euthyroid and hypothyroid rats at PND12, but the situation in the hippocampus was not examined. Such differences in TH-dependency of KCC2 expression may reflect the highly heterogeneous nature of the timing and strength of TH signaling in the developing brain (Quignodon et al., 2004).

Another characteristic of KCC2 protein expression in the developing hippocampus was the presence of a second phase of robust increase between PND15 and 28 which was not dependent on TH (Fig. 8B). Since KCC2 expression is shown to be up-regulated by brain-derived neurotrophic factor (BDNF) during development

(Aguado et al., 2003; Blaesse et al., 2009), this latter phase of increase may be regulated by the activity-dependent up-regulation of BDNF. In this context, recent studies on the expression of KCC2 in the adult after brain injury have revealed an interesting interplay between TH and BDNF on GABAergic neurotransmission (Shulga et al., 2009; Shulga and Rivera, 2013). In contrast to the situation during development, BDNF down-regulates KCC2 in mature neurons under both physiological and pathological conditions, resulting in reversal of GABA(A) responses toward depolarization (Payne et al., 2003; Rivera et al., 2004; Shulga et al., 2009). A recent study on lesioned hippocampal slices, however, has demonstrated that thyroxin up-regulates the expression of KCC2 in injured neurons independent of BDNF. The level of TH which is high during development and becomes lower after maturation may thus be a critical factor in setting the direction of BDNF action on KCC2 expression.

TH is thus found to be essential not only for the development of the presynaptic GABAergic neurons and their terminals but also for the maturation of the postsynaptic GABAergic system, and one of the primary targets of TH seems to be the K^+/Cl^- co-transporter, KCC2. Apart from its function as a transporter, recent studies revealed a critical role of KCC2 in both the formation (Li et al., 2007) and functional maintenance (Gauvain et al., 2011) of glutamatergic synapses through interaction with the submembranous actin cytoskeleton. Reduction of KCC2 in the hypothyroid hippocampus thus influences also synaptic efficacy at glutamatergic synapses.

A variety of behavioral deficits have been described in hypothyroid animals, some of which implicate impairment of hippocampal function such as memory impairment and learning disorder (Akaike et al., 1991; Smith et al., 2002; Venero et al., 2005) and a reduction in seizure susceptibility (Hadjab-Lallemend et al., 2010). Impairments in the development and maturation of the GABAergic system may thus be essential factors involved in such disorders caused by hypothyroidism.

Acknowledgements

References

Aguado, F., Carmona, M.A., Pozas, E., Aguiló, A., Martínez-Guijarro, F.J., Alcantara, S., Borrell, V., Yuste, R., Ibañez, C.F., Soriano, E., 2003. BDNF regulates spontaneous correlated activity at early developmental stages by increasing synaptogenesis and expression of the K+/Cl− co-transporter KCC2. Development 130, 1267–1280.

Akaike, M., Kato, N., Ohno, H., Kobayashi, T., 1991. Hyperactivity and spatial maze learning impairment of adult rats with temporary neonatal hypothyroidism. Neurotoxicol. Teratol. 13, 317–322.

Ben-Ari, Y., 2002. Excitatory actions of GABA during development: the nature of the nurture. Nat. Rev. Neurosci. 3, 728–739.

Ben-Ari, Y., Gaiarsa, J.L., Tyzio, R., Khazipov, R., 2007. GABA: a pioneer transmitter that excites immature neurons and generates primitive oscillations. Physiol. Rev. 87, 1215–1284.

Bernal, J., Nunez, J., 1995. Thyroid hormones and brain development. Eur. J. Endocrinol. 133, 390–398.

Blaesse, P., Airaksinen, M.S., Rivera, C., Kaila, K., 2009. Cation-chloride cotransporters and neuronal function. Neuron 61, 820–838.

Bradley, D.J., Towle, H.C., Young 3rd, W.S., 1992. Spatial and temporal expression of alpha- and beta-thyroid hormone receptor mRNAs, including the beta 2-subtype, in the developing mammalian nervous system. J. Neurosci. 12 (6), 2288–2302.

Chard, P.S., Bleakman, D., Christakos, S., Fullmer, C.S., Miller, R.J., 1993. Calcium buffering properties of calbindin D28k and parvalbumin in rat sensory neurones. J. Physiol. 472, 341–357.

Chatonnet, F., Guyot, R., Picou, F., Bondesson, M., Flamant, F., 2012. Genome-wide search reveals the existence of a limited number of thyroid hormone receptor alpha target genes in cerebellar neurons. PLoS One 7 (5), e30703.

Dong, H., Yauk, C.L., Rowan-Carroll, A., You, S.H., Zoeller, R.T., Lambert, I., Wade, M.G., 2009. Identification of thyroid hormone receptor binding sites and target genes using ChIP-on-chip in developing mouse cerebellum. PLoS One 4 (2), e4610.

Erlander, M.G., Tillakaratne, N.J., Feldblum, S., Patel, N., Tobin, A.J., 1991. Two genes encode distinct glutamate decarboxylases. Neuron 7, 91–100.

Esclapez, M., Tillakaratne, N.J., Kaufman, D.L., Tobin, A.J., Houser, C.R., 1994. Comparative localization of two forms of glutamic acid decarboxylase and their mRNAs in rat brain supports the concept of functional differences between the forms. J. Neurosci. 14, 1834–1855.

Farrant, M., Kaila, K., 2007. The cellular, molecular and ionic basis of GABA(A) receptor signalling. Prog. Brain Res. 160, 59–87.

Farsetti, A., Mitsuhashi, T., Desvergne, B., Robbins, J., Nikodem, V.M., 1991. Molecular basis of thyroid hormone regulation of myelin basic protein gene expression in rodent brain. J. Biol. Chem. 266, 23226–23232.

Fiumelli, H., Woodin, M.A., 2007. Role of activity-dependent regulation of neuronal chloride homeostasis in development. Curr. Opin. Neurobiol. 17, 81–86.

Friauf, E., Wenz, M., Oberhofer, M., Nothwang, H.G., Balakrishnan, V., Knipper, M., Löhrke, S., 2008a. Hypothyroidism impairs chloride homeostasis and onset of inhibitory neurotransmission in developing auditory brainstem and hippocampal neurons. Eur. J. Neurosci. 28 (12), 2371–2380.

Friauf, E., Wenz, M., Oberhofer, M., Nothwang, H.G., Balakrishnan, V., Knipper, M., Löhrke, S., 2008b. Hypothyroidism impairs chloride homeostasis and onset of inhibitory neurotransmission in developing auditory brainstem and hippocampal neurons. Eur. J. Neurosci. 28, 2371–2380.

Friesema, E.C., Ganguly, S., Abdalla, A., Manning Fox, J.E., Halestrap, A.P., Visser, T.J., 2003. Identification of monocarboxylate transporter 8 as a specific thyroid hormone transporter. J. Biol. Chem. 278, 40128–40135.

Fukuda, T., Aika, Y., Heizmann, C.W., Kosaka, T., 1998. GABAergic axon terminals at perisomatic and dendritic inhibitory sites show different immunoreactivities against two GAD isoforms, GAD67 and GAD65, in the mouse hippocampus: a digitized quantitative analysis. J. Comp. Neurol. 395, 177–194.

Fukuda, T., Heizmann, C.W., Kosaka, T., 1997. Quantitative analysis of GAD65 and GAD67 immunoreactivities in somata of GABAergic neurons in the mouse hippocampus proper (CA1 and CA3 regions), with special reference to parvalbumin-containing neurons. Brain Res. 764, 237–243.

Gauvain, G., Chamma, I., Chevy, Q., Cabezas, C., Irinopoulou, T., Bodrug, N., Carnaud, M., Lévi, S., Poncer, J.C., 2011. The neuronal K-Cl cotransporter KCC2 influences postsynaptic AMPA receptor content and lateral diffusion in dendritic spines. Proc. Natl. Acad. Sci. U.S.A. 108, 15474–15479.

Gilbert, M.E., Sui, L., Walker, M.J., Anderson, W., Thomas, S., Smoller, S.N., Schon, J.P., Phani, S., Goodman, J.H., 2007. Thyroid hormone insufficiency during brain development reduces parvalbumin immunoreactivity and inhibitory function in the hippocampus. Endocrinology 148, 92–102.

Guadaño-Ferraz, A., Benavides-Piccione, R., Venero, C., Lancha, C., Vennström, B., Sandi, C., DeFelipe, J., Bernal, J., 2003. Lack of thyroid hormone receptor alpha1 is associated with selective alterations in behavior and hippocampal circuits. Mol. Psychiatry 8, 30–38.

Guadaño-Ferraz, A., Obregón, M.J., St Germain, D.L., Bernal, J., 1997. The type 2 iodothyronine deiodinase is expressed primarily in glial cells in the neonatal rat brain. Proc. Natl. Acad. Sci. U.S.A. 94, 10391–10396.

Gutiérrez, R., Romo-Parra, H., Maqueda, J., Vivar, C., Ramìrez, M., Morales, M.A., Lamas, M., 2003. Plasticity of the GABAergic phenotype of the "glutamatergic" granule cells of the rat dentate gyrus. J. Neurosci. 23 (13), 5594–5598.

Hadjab-Lallemend, S., Wallis, K., van Hogerlinden, M., Dudazy, S., Nordström, K., Vennström, B., Fisahn, A., 2010. A mutant thyroid hormone receptor alpha1 alters hippocampal circuitry and reduces seizure susceptibility in mice. Neuropharmacology 58 (7), 1130–1139.

Heuer, H., Maier, M.K., Iden, S., Mittag, J., Friesema, E.C., Visser, T.J., Bauer, K., 2005. The monocarboxylate transporter 8 linked to human psychomotor retardation is highly expressed in thyroid hormone-sensitive neuron populations. Endocrinology 146, 1701–1706.

Koibuchi, N., Chin, W.W., 2000. Thyroid hormone action and brain development. Trends Endocrinol. Metab. 11, 123–128.

Li, H., Khirug, S., Cai, C., Ludwig, A., Blaesse, P., Kolikova, J., Afzalov, R., Coleman, S.K., Lauri, S., Airaksinen, M.S., Keinänen, K., Khiroug, L., Saarma, M., Kaila, K.,

Rivera, C., 2007. KCC2 interacts with the dendritic cytoskeleton to promote spine development. Neuron 56, 1019–1033.

Manzano, J., Cuadrado, M., Morte, B., Bernal, J., 2007. Influence of thyroid hormone and thyroid hormone receptors in the generation of cerebellar GABAergic interneurons from precursor cells. Endocrinology 148, 5746–5751.

Martínez de Arrieta, C., Morte, B., Coloma, A., Bernal, J., 1999. The human RC3 gene homolog, NRGN contains a thyroid hormone-responsive element located in the first intron. Endocrinology 140, 335–343.

Muñoz, A., Rodriguez-Peña, A., Perez-Castillo, A., Ferreiro, B., Sutcliffe, J.G., Bernal, J., 1991. Effects of neonatal hypothyroidism on rat brain gene expression. Mol. Endocrinol. 5, 273–280.

Oppenheimer, J.H., Schwartz, H.L., 1997. Molecular basis of thyroid hormone-dependent brain development. Endocr. Rev. 18, 462–475.

Payne, J.A., Rivera, C., Voipio, J., Kaila, K., 2003. Cation-chloride co-transporters in neuronal communication, development and trauma. Trends Neurosci. 26, 199–206.

Quignodon, L., Grijota-Martinez, C., Compe, E., Guyot, R., Allioli, N., Laperrière, D., Walker, R., Meltzer, P., Mader, S., Samarut, J., Flamant, F., 2007. A combined approach identifies a limited number of new thyroid hormone target genes in post-natal mouse cerebellum. J. Mol. Endocrinol. 39 (1), 17–28.

Quignodon, L., Legrand, C., Allioli, N., Guadano-Ferraz, A., Bernal, J., Samarut, J., Flamant, F., 2004. Thyroid hormone signaling is highly heterogeneous during pre- and postnatal brain development. J. Mol. Endocrinol. 33, 467–476.

Rivera, C., Voipio, J., Payne, J.A., Ruusuvuori, E., Lahtinenn, H., Lamsa, K., Pirvola, U., Saarma, M., Kaila, K., 1999. The K⁺/Cl⁻ co-transporter KCC2 renders GABA hyperpolarizing during neuronal maturation. Nature 397, 251–255.

Rivera, C., Voipio, J., Thomas-Crusells, J., Li, H., Emri, Z., Sipilä, S., Payne, J.A., Minichiello, L., Saarma, M., Kaila, K., 2004. Mechanism of activity-dependent downregulation of the neuron-specific K-Cl cotransporter KCC2. J. Neurosci. 24, 4683–4691.

Shulga, A., Blaesse, A., Kysenius, K., Huttunen, H.J., Tanhuanpää, K., Saarma, M., Rivera, C., 2009. Thyroxin regulates BDNF expression to promote survival of injured neurons. Mol. Cell Neurosci. 42, 408–418.

Shulga, A., Rivera, C., 2013. Interplay between thyroxin, BDNF and GABA in injured neurons. Neuroscience 3 (239), 241–252.

Sloviter, R.S., Dichter, M.A., Rachinsky, T.L., Dean, E., Goodman, J.H., Sollas, A.L., Martin, D.L., 1996. Basal expression and induction of glutamate decarboxylase and GABA in excitatory granule cells of the rat and monkey hippocampal dentate gyrus. J. Comp. Neurol. 373 (4), 593–618.

Smith, J.W., Evans, A.T., Costall, B., Smythe, J.W., 2002. Thyroid hormones, brain function and cognition: a brief review. Neurosci. Biobehav. Rev. 26, 45–60.

Takahashi, M., Kondoh, Y., Tashiro, H., Koibuchi, N., Kuroda, Y., Tashiro, T., 2005. Monitoring synaptogenesis in the developing mouse cerebellum with an original oligonucleotide microarray. J. Neurosci. Res. 80 (6), 777–788.

Takahashi, M., Negishi, T., Tashiro, T., 2008. Identification of genes mediating thyroid hormone action in the developing mouse cerebellum. J. Neurochem. 104 (3), 640–652.

Thompson, C.C., Bottcher, M.C., 1997. The product of a thyroid hormone-responsive gene interacts with thyroid hormone receptors. Proc. Natl. Acad. Sci. U.S.A. 94 (16), 8527–8532.

Thompson, C.C., Potter, G.B., 2000. Thyroid hormone action in neural development. Cereb. Cortex 10, 939–945.

Venero, C., Guadaño-Ferraz, A., Herrero, A.I., Nordström, K., Manzano, J., de Escobar, G.M., Bernal, J., Vennström, B., 2005. Anxiety, memory impairment, and locomotor dysfunction caused by a mutant thyroid hormone receptor alpha1 can be ameliorated by T3 treatment. Genes Dev. 19, 2152–2163.

Wallis, K., Sjogren, M., von Hogerlinden, M., Silberberg, G., Fisahn, A., Nordstrom, K., Larsson, L., Westerblad, H., de Escobar, G.M., Shupliakov, O., Vennstron, B., 2008. Locomoter deficiencies and aberrant development of subtype-specific GABAergic Interneurons caused by an unliganded thyroid hormone receptor α1. J. Neurosci. 28, 1904–1915.

Westerholz, S., de Lima, A.D., Voigt, T., 2010. Regulation of early spontaneous network activity and GABAergic neurons development by thyroid hormone. Neuroscience 168 (2), 573–589.

Wiens, S.C., Trudeau, V.L., 2006. Thyroid hormone and g-aminobutyric acid (GABA) interactions in neuroendocrine systems. Comp. Biochem. Physiol. A 144, 332–344.

Williams, G.R., 2008. Neurodevelopmental and neurophysiological actions of thyroid hormone. J. Neuroendocrinol. 20, 784–794.

Alterations in Local Thyroid Hormone Signaling in the Hippocampus of the SAMP8 Mouse at Younger Ages: Association With Delayed Myelination and Behavioral Abnormalities

Erika Sawano,[1] Takayuki Negishi,[1] Tomoyuki Aoki,[2] Masami Murakami,[2] and Tomoko Tashiro[1]*

[1]Department of Chemistry and Biological Science, Aoyama Gakuin University, Sagamihara, Kanagawa, Japan
[2]Department of Clinical Laboratory Medicine, Gunma University Graduate School of Medicine, Maebashi, Japan

The senescence-accelerated mouse (SAM) strains were established through selective inbreeding of the AKR/J strain based on phenotypic variations of aging and consist of senescence-prone (SAMP) and senescence-resistant (SAMR) strains. Among them, SAMP8 is considered as a model of neurodegeneration displaying age-associated learning and memory impairment and altered emotional status. Because adult hypothyroidism is one of the common causes of cognitive impairment and various psychiatric disorders, we examined the possible involvement of thyroid hormone (TH) signaling in the pathological aging of SAMP8 using the senescence-resistant SAMR1 as control. Although plasma TH levels were similar in both strains, a significant decrease in type 2 deiodinase (D2) gene expression was observed in the SAMP8 hippocampus from 1 to 8 months of age, which led to a 35–50% reductions at the protein level and 20% reduction of its enzyme activity at 1, 3, and 5 months. D2 is responsible for local conversion of thyroxine into transcriptionally active 3,5,3'-triiodothyronine (T3), so the results suggest a reduction in T3 level in the SAMP8 hippocampus. Attenuation of local TH signaling was confirmed by downregulation of TH-dependent genes and by immunohistochemical demonstration of delayed and reduced accumulation of myelin basic protein, the expression of which is highly dependent on TH. Furthermore, we found that hyperactivity and reduced anxiety were not age-associated but were characteristic of young SAMP8 before they start showing impairments in learning and memory. Early alterations in local TH signaling may thus underlie behavioral abnormalities as well as the pathological aging of SAMP8. © 2012 Wiley Periodicals, Inc.

Key words: thyroid hormone; SAMP8; type 2 deiodinase; hippocampus; hyperactivity; myelin basic protein

The senescence-accelerated mouse (SAM) strains were established through selective inbreeding of the AKR/J strain based on phenotypic variations of accelerated aging, such as amyloidosis, osteoporosis, and learning and memory deficits (Takeda et al., 1981). They consist of senescence-prone (SAMP) strains, which exhibit accelerated aging with a shorter life span, and senescence-resistant (SAMR) strains, which show normal aging. Among the SAMP strains, the SAMP8 strain displays mainly age-associated impairments in CNS function, including marked deficits in learning and memory (Miyamoto et al., 1986; Flood and Morley, 1992, 1993; Yagi et al., 1998), altered emotional status (Miyamoto et al., 1992; Markowaska et al., 1998), and abnormality of circadian rhythm (Miyamoto et al., 1986; Colas et al., 2005), with relatively mild physical impairments. Neuropathological and neurochemical studies have further shown that pathological changes observed in the aged brain such as increased oxidative stress, occurrence of Aβ-immunoreactive deposits (Del Valle et al., 2010), and neuroinflammation are detected earlier and at increased severity in the SAMP8 brain, especially in the

hippocampus, confirming the usefulness of this strain as a model for neurodegeneration (for review see Butterfield and Poon, 2005; Takeda, 2009; Tomobe and Nomura, 2009). The causes for such accelerated senescence, however, remain to be elucidated.

We focused on the thyroid hormone (TH) signaling as one potential contributing factor to accelerated aging in SAMP8, because TH plays essential roles not only in the developing brain (Oppenheimer and Schwartz, 1997; Koibuchi and Chin, 2000; Bernal, 2005; Williams, 2008) but also in the mature brain to maintain its proper functions. Adult hypothyroidism is one of the most common causes of transient dementia, and thyroid disorders have been linked to various psychiatric and neuropsychological disorders, including learning deficits, impaired attention, anxiety, and depression (for review see Davis and Tremont, 2007).

TH exerts its effects mainly through binding to the specific nuclear receptors of the steroid-retinoic acid–TH receptor superfamily, which function as ligand-regulated transcription factors (Oppenheimer and Schwartz, 1997; Koibuchi and Chin, 2000; Williams, 2008). The transcriptionally active form of TH that binds to these receptors is 3,5,3'-triiodothyronine (T3) produced by enzymatic deiodination of the initially synthesized form, thyroxine (T4). In addition to the well-known feedback system consisting of hypothalamus, pituitary, and thyroid gland (the HPT axis), which regulates the production of T4, it is now established that the concentration of T3 is locally regulated by three types of iodothyronine deiodinases; type 1 and 2 deiodinases (D1, D2), which convert T4 into active T3, and type 3 deiodinase (D3), which inactivates T3 (Gereben et al., 2008; Dentice and Salvatore, 2011). The T3-producing enzyme in the CNS is D2, which is expressed in astrocytes, whereas D3 is expressed in neurons.

In the present study, we examined the expression of D2 and D3 as well as representative TH-dependent genes to evaluate the local T3 availability in the hippocampus of SAMP8. The results indicate that, in spite of normal plasma TH level, the local TH signaling was significantly attenuated in the SAMP8 hippocampus from an early age (1 month) because of a significant reduction in D2 activity caused by a decrease at both mRNA and protein levels. At the same time, we found that, unlike the previously described behavioral abnormalities of SAMP8, hyperactivity and reduced anxiety were not age-associated but were characteristic of young SAMP8 (1–5 months), before they start showing symptoms of learning and memory impairment. Reduced local TH signaling starting during development may thus be a cause of abnormal behavior as well as accelerated aging of SAMP8.

MATERIALS AND METHODS
Animals

Male SAMP8 and SAMR1 mice were purchased from SLC (Shizuoka, Japan). They were housed individually under controlled temperature (24°C ± 1°C) on a 12-hr-light (06:00–18:00 hr):12-hr-dark (18:00–06:00 hr) cycle. Food and water were available ad libitum. To determine optimal conditions for the measurement of hippocampal iodothyronine deiodinase activity, 1-month-old male ICR mice (SLC) were used. All animal treatments were approved by the Animal Experimentation Committee of Aoyama Gakuin University and were carried out under veterinary supervision and in accordance with the Society for Neuroscience Guidelines for the use of animals in neuroscience research.

For one series of experiments, six mice each of SAMR1 and SAMP8 strains were used at 1, 3, 5, 8, and 10 months of age. After the behavioral tests described below, they were sacrificed under deep ether anesthesia. Blood samples were drawn from the heart and collected with EDTA as anticoagulant. After perfusion with phosphate-buffered saline (PBS), the brains were removed and separated sagitally into halves. In total five series of animals were used to obtain tissue samples for mRNA and protein extractions, measurement of enzyme activity, and immunohistochemical observation. For mRNA and protein extractions and enzyme activity measurements, hippocampi were removed, immediately frozen in liquid N_2, and kept at −80°C until use. For immunohistochemistry, brain halves were immediately fixed in 4% paraformaldehyde (PFA).

Passive Avoidance Test

Learning and memory abilities of SAMP8 and SAMR1 mice were examined at 1, 3, 5, 8, and 10 months by passive avoidance test using a two-compartment (light and dark) step-through cage (Muromachi Kikai Co., Tokyo, Japan). The tests were conducted between 6:00 and 10:00 PM. On the first day of examination (day 1), each mouse was placed in the light compartment, and the latency before entering the dark compartment (up to 60 sec) was measured. The mouse received an electrical shock (0.5 mA, 1 sec) immediately after entering the dark compartment. These trials were repeated up to five times until each mouse had learned to stay in the light compartment for at least 60 sec. On the next day (day 2), each mouse was placed in the light compartment, and the latency before entering the dark compartment (up to 300 sec) was measured.

Open-Field Test

Behavior and locomotor activity of SAMP8 and SAMR1 mice were examined at 1, 3, 5, 8 and 10 months by open-field test in a rectangular field (60 cm × 90 cm with walls of 45 cm height) with which all animals were unfamiliar. The tests were conducted between 6:00 and 10:00 PM. Each mouse was placed in the center of the field, and its behavior and locomotor activity were monitored for 5 min using a video camera and computerized analysis system (Smart System; Panlab, Barcelona, Spain).

Measurement of Plasma T4 and T3 Levels

Blood samples were centrifuged at 1,500g for 20 min at room temperature to obtain the plasma as the supernatant. T4 and T3 in the plasma from SAMP8 (n = 6) and SAMR1

TABLE I. Primers for Real-Time Quantitative PCR

	Forward	Reverse
ppia	GCAAGACCAGCAAGAAGATCACC	CTTCAGTGAGAGCAGAGATTACAG
dio2	CTACTACCTATGATCTGATTAAGTG	GGCTGGAACTAACACTTCAGTCC
dio3	CGACTACGCACAAGGGACCCG	CGATGTAGATGATAAGGAAGTCAAC
thra	CACCCCTATACACACAGAGAGC	GCCAAGCCAAGCCAAGCCAAG
thrb	CTATGACCCAGACAGCGAGACTC	CAGAGACATGCCCAGGTCAAAG
mct8	CATTCACAGGTCCCAGATCTGCCC	GCCCACACGTGCACACACGC
rc3	GACTTCCCTACTGTGTTTGTGAG	CTACGCCACGACGAAGCCAGC
hr	GCTGACCCCTCCCCTCATGG	GCAGTTGAGATACACAGAGGAAG
mbp	GGCACAGAGACACGGGCATCC	GCGACTTCTGGGGCAGGGAGC
enpp2	GTCAGAAAGGAATGGGGTCAACG	AGTGGGTAGGGACAGGAATAGAG

(n = 6) were measured by competitive enzyme-linked immunosorbent assay (ELISA) kit (Diagnostic Automation Inc.) according to the protocols recommended by the manufacturer.

Real-Time Quantitative Fluorescence-Based PCR

Total RNA was prepared individually from each hippocampus obtained from six mice of both strains at 1, 3, 5, 8, and 10 months using Trizol reagent (Invitrogen Life Technologies, Carlsbad, CA). The integrity of RNA samples was routinely monitored by microcapillary electrophoresis using a Bioanalyzer 2100 (Agilent Technologies, Palo Alto, CA). First-strand cDNA was synthesized from 1 μg total RNA from one animal using SuperScript III reverse transcription kit (Invitrogen Life Technologies). Expression levels of the following 10 genes in cDNA samples were quantified by fluorescence-based real-time PCR using Step One (Applied Biosystems, Foster City, CA) with SYBR Premix ExTaq (Takara, Shiga, Japan): cyclophilin-A (*ppia*), type 2 deiodinase (*dio2*), type 3 deiodinase (*dio3*), monocarboxylic acid transporter 8 (*mct8*), thyroid hormone receptor α (*thra*), thyroid hormone receptor β (*thrb*), neurogranine (*rc3*), hairless (*hr*), myelin basic protein (*mbp*), and ectonucleotide pyrophosphatase/phosphodiesterase 2 (*enpp2*). Cyclophilin-A (*ppia*) was used as an internal standard gene. PCR primers were designed in Oligo 6.0 primer analysis software (Molecular Biology Insights; Takahashi et al., 2008). Sequences of the PCR primers are listed in Table I.

Western Blotting

Each hippocampal sample obtained from SAMP8 or SAMR1 at 1, 3, 5, 8, and 10 months (n = 5–8 for either strain at each time point) was homogenized in 10 volumes of SDS sample buffer (0.06 M Tris-HCl, pH 6.8, 10% glycerol, 2% SDS, 0.04% bromophenol blue, 2% β-mercaptoethanol) containing protease inhibitors (Complete Mini EDTA-Free Protease Inhibitor Cocktail and PhosSTOP Phosphatase Inhibitor Cocktail; Roche Applied Science, Indianapolis, IN) using a glass-Teflon homogenizer, boiled at 100°C for 5 min, and centrifuged at 15,000g for 10 min at RT. Supernatants containing extracted proteins were collected and separated by SDS-PAGE on Tris-HCl gels followed by electrophoretic transfer onto polyvinyl difluoride (PVDF) membranes (Millipore, Bedford, MA). The blots were blocked for 1 hr at RT with 2% bovine serum albumin (BSA) or 2.5% skimmed

milk in PBS containing 0.1% Tween 20 (PBS-T) and 0.02% sodium azide and incubated overnight at 4°C with one of the following primary antibodies in 2% BSA and 0.02% sodium azide-containing PBS: rabbit polyclonal anti-type 2 deiodinase (D2; 1:1,000; Abcam, Cambridge, United Kingdom), rabbit polyclonal anti-type 3 deiodinase (D3; 1:2,000; Novus Biologicals, Littleton, CO), chicken polyclonal anti-glial fibrillary acidic protein (GFAP; 1:20,000; Abcam), and monoclonal anti-β-actin (1:10,000; Sigma, St. Louis, MO). After being rinsed in PBS-T, the blots were incubated for 1 hr at RT with either of the following horseradish peroxidase (HRP)-conjugated secondary antibodies in 2% BSA with 0.02% sodium azide: anti-rabbit IgG (1:5,000), anti-chicken IgY (1:5,000), and anti-mouse IgG (1:10,000; all from Jackson Immunoresearch, West Grove, PA). The blots were rinsed several times in PBS-T and visualized by exposure to Hyperfilm ECL (GE Healthcare, Buckinghamshire, United Kingdom) using an Immobilon Western Chemiluminescent HRP Substrate (Millipore). For quantification, the films were scanned, and the density of each band was measured in Image J (National Institutes of Health).

Measurement of Iodothyronine Deiodinase Activity

Iodothyronine deiodinase activity was measured as previously described (Murakami et al., 1988), with minor modifications. To determine optimal conditions for the measurement of hippocampal D2 activity, iodothyronine deiodinase activity in the hippocampus of 1-month-old ICR mice was first characterized. Hippocampal samples were homogenized in homogenizing buffer (100 mM potassium phosphate, pH 7.0, containing 1 mM EDTA and 20 mM dithiothreitol) and centrifuged at 1,500g for 15 min at 4°C. The supernatants were incubated in a total volume of 50 μl containing various concentrations of [^{125}I]T4 (NEN Life Science Products Corp., Boston, MA), which was purified using LH-20 (Pharmacia Biotech, Uppsala, Sweden) column chromatography on the day of experiment, 1 mM EDTA, 20 mM dithiothreitol, in the presence or absence of 1 mM 6-propyl-2-thiouracil (PTU) or 1 mM iopanoic acid for 2 hr at 37°C. The reaction was terminated by adding 100 μl ice-cold 2% BSA and 800 μl ice-cold 10% trichloroacetic acid. After centrifugation at 1,500g for 10 min at 4°C, the supernatant was applied to a small column packed with AG 50W-X2 resin (bed volume 1 ml; Bio-Rad Laboratories, Hercules, CA) and then eluted with 2 ml of 10% glacial acetic acid. Separated ^{125}I was
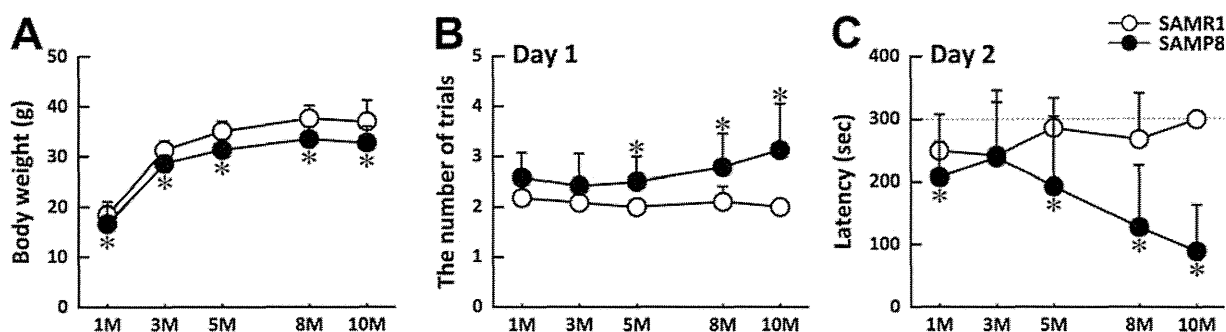
Fig. 1. Body weights and cognitive performances of SAMP8 and SAMR1 mice between 1 and 10 months. **A:** Body weights of SAMP8 (solid circles) and SAMR1 (open circles). **B,C:** Comparison of learning and memory abilities of SAMP8 (solid circles) and SAMR1 (open circles) by passive avoidance test at different ages. On day 1 (B), number of trials required before each mouse learned to stay in the light compartment for 60 sec was counted. On day 2 (C), latency time before each mouse entered the dark compartment (up to 300 sec) was measured. Results are expressed as means + SD. A: n = 21–59 (SAMR1), n = 14–55 (SAMP8). B,C: n = 8–15 (SAMR1), n = 8–12 (SAMP8). *$P < 0.05$ between age-matched SAMP8 and SAMR1.

counted with a γ-counter. Nonenzymatic deiodination was corrected by subtracting I^- released in control tubes without homogenized samples. The protein concentration was determined by Bradford's method with BSA as a standard (Bradford, 1976). The deiodinating activity was calculated as fmol I^- released/mg protein/min, after multiplication by a factor of 2 to correct for random labeling at the equivalent 3′ and 5′ positions.

Each hippocampal sample from SAMP8 or SAMR1 was homogenized in 10 volumes of homogenizing buffer and centrifuged at 1,500g for 15 min at 4°C. Resultant supernatants were used for the measurement of D2 activity in the presence of 2 nM [^{125}I]T4, 1 mM EDTA, 20 mM dithiothreitol, and 1 mM PTU, as described above.

Immunohistochemistry

For immunohistochemical analysis, brain samples were fixed in 4% PFA for 48 hr at 4°C, dehydrated, embedded in paraffin, and cut into 8-μm-thick coronal sections. After deparaffinization and rehydration, the sections were incubated in 0.5% H_2O_2 for 20 min at RT to quench endogenous peroxidase activity, followed by 0.2% Triton X-100 for 15 min at RT. They were rinsed and incubated in 4% BSA for 30 min at RT to block nonspecific binding sites. Monoclonal anti-MBP antibody (1:1,000; Millipore) or monoclonal anti-S100 calcium binding protein B (S100β; 1:1,000; Sigma) was then applied to each section, and the sections were incubated overnight at 4°C. They were further rinsed and incubated with biotinylated secondary antibody (anti-mouse IgG; Chemicon/Millipore) at a dilution of 1:5,000 in BSA/PBS for 1 hr at RT. The sections were incubated in biotin-conjugated horseradish peroxidase with streptoavidin (ABC Elite Kit; Vector, Burlingame, CA) at a dilution of 1:1,000 for 30 min at RT and then visualized with nickel-intensified diaminobenzidine. The sections were counterstained with Carazzi's hematoxylin (Wako, Osaka, Japan), dehydrated and mounted in Entellan New (Merck, Darmstadt, Germany), and observed with a microscope (Axioplan 2; Carl Zeiss, Oberkochen, Germany).

Statistical Analysis

All numerical data were expressed as mean ± SD and analyzed by one-way ANOVA. When ANOVA revealed significant differences, it was followed by two-tailed Student's t-test. The level of significance was set at $P < 0.05$.

RESULTS

Confirmation of the Age-Associated Cognitive Impairment in SAMP8 Mice

SAMP8 mice were active and showed little physical impairment during the observation period of up to 10 months. They had slightly lower body weights (8.5–11.5%) compared with the age-matched SAMR1 (Fig. 1A). Progressive decline in learning and memory abilities of SAMP8 mice was confirmed by passive avoidance conditioning as shown in Figure 1B,C. Average number of trials necessary for learning on the first day of trial was significantly greater in SAMP8 mice compared with SAMR1 at 5, 8, and 10 months of age (125.0% at 5 months, 126.6% at 8 months, and 156.3% at 10 months of age-matched SAMR1), whereas memory retention represented by the latency before entering the dark compartment on the second day was progressively decreased in SAMP8 mice between 5 and 10 months (67.5% at 5 months, 48.6% at 8 months, and 29.9% at 10 months of age-matched SAMR1). Both of these parameters remained constant in SAMR1 between 1 and 10 months, indicating that SAMP8 mice became progressively impaired in learning and memory starting at about 5 months.

Behavioral Abnormalities of SAMP8 Mice Observed Prior to the Onset of Cognitive Decline

In addition to cognitive impairment, SAMP8 mice have been reported to exhibit behavioral abnormalities such as reduced anxiety that were also age dependent (Miyamoto et al., 1992; Markowska et al., 1998). With
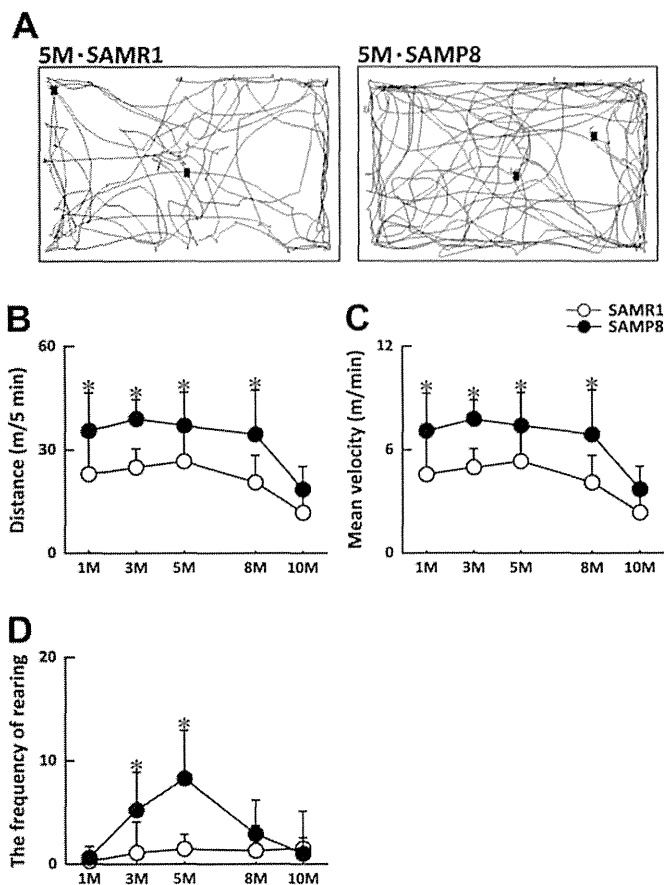
A

5M·SAMR1   5M·SAMP8

B

C

D

Fig. 2. Behavioral comparison of SAMP8 and SAMR1 mice by open-field test at different ages. **A:** Typical examples of trajectories of 5-month-old SAMR1 and SAMP8 in the first 5 min in an unfamiliar environment. Total distance (**B**), mean velocity during movement (**C**), and the frequency of rearing in the central part of the open field (**D**), recorded during the 5 min of test session. Results are expressed as means + SD [n = 13–30 for 1–8 months, n = 8 for 10 months (SAMR1), n = 10–28 for 1–8 months, n = 5 for 10 months (SAMP8)]. *$P < 0.05$ between age-matched SAMP8 and SAMR1.

the open-field test, however, we noted hyperactivity and reduced anxiety in young SAMP8 mice before they started showing cognitive decline, as shown in Figure 2. Typical examples of trajectories during the first 5 min of the test session in an unfamiliar environment are shown in Figure 2A for SAMR1 and SAMP8 at 5 months. Measurement of total distance traveled during the first 5 min demonstrated a significant increase in SAMP8 mice at 1, 3, 5, and 8 months compared with SAMR1 (Fig. 2B). Mean velocity during movement was also higher by ~30% in SAMP8 (Fig. 2C). In addition to such hyperactivity, rearing in the central part of the open field, interpreted as a sign of reduced anxiety, was frequently observed with SAMP8 mice at 3 and 5 months (Fig. 2D), whereas the frequency of rearing was minimal with SAMR1 at all ages.

TABLE II. Plasma Levels of Thyroxine (T4) and 3,5,3′-Triiodothyronine (T3) in SAMP8 and SAMR1 at Different Ages*

Age (months)	T4 (ng/ml)		T3 (ng/ml)	
	SAMR1	SAMP8	SAMR1	SAMP8
1	103.1 ± 14.4	109.4 ± 12.2	9.9 ± 0.7	9.4 ± 1.2
3	115.0 ± 15.0	103.5 ± 10.4	10.4 ± 0.7	10.9 ± 0.1
5	103.6 ± 20.3	115.8 ± 17.1	10.7 ± 0.2	10.4 ± 0.4
8	118.8 ± 19.1	98.4 ± 11.2	10.3 ± 1.7	10.8 ± 0.1
10	83.8 ± 15.9	110.3 ± 9.2	10.9 ± 0.2	10.6 ± 0.4

*Values are expressed as means ± SD [n = 6 (SAMR1), n = 6 (SAMP8)]. Plasma levels of T4 and T3 were comparable in the two strains at all ages examined.

Differences in the Expression of Genes Involved in Local TH Metabolism and Signaling in the Hippocampus of SAMP8 and SAMR1 Mice

To examine the possible involvement of TH signaling in the cognitive impairment and abnormal behaviors of SAMP8 mice, we first compared plasma TH levels of SAMP8 and SAMR1. As shown in Table II, plasma levels of T4 and T3 determined by ELISA were similar in both strains at all ages examined (1–10 months), indicating that the systemic TH status was not altered in SAMP8.

Because the level of transcriptionally active T3 in the CNS has been shown to be regulated locally, we next examined the expression of genes regulating local T3 availability as well as genes for its receptors in the hippocampus of SAMP8 and SAMR1 at different ages by real-time PCR. As shown in Figure 3A,B, significant differences between the two strains were observed in the mRNA expression of the two enzymes regulating the local T3 level. In the SAMP8 hippocampus, expression of the D2 gene (dio2), which converts T4 into active T3, was significantly downregulated at 1, 3, 5, and 8 months (Fig. 3A), whereas that of the D3 gene (dio3), responsible for inactivation of T3, showed a tendency to be upregulated (Fig. 3B) in comparison with SAMR1. The major neuronal TH transporter, monocarboxylate anion transporter 8 (mct8), was also significantly downregulated in SAMP8 at 3 months (Fig. 3C).

The mRNA expression of TH receptor α (thra) was similar in both strains at all time points (Fig. 3D), whereas TH receptor β (thrb) was significantly downregulated at 1 month and upregulated at 8 and 10 months in SAMP8 (Fig. 3E). Both of these TH receptors as well as dio2 and dio3 showed a peak of expression at 3 months, suggesting the importance of TH signaling at the maturation stage.

Reduction in D2 Protein and D2 Activity in the Hippocampus of SAMP8

Sustained reduction of dio2 mRNA between 1 month and 5 months resulted in 35–50% reduction of the D2 protein in the hippocampus of SAMP8 compared with SAMR1 throughout the observation period, as shown in Figure 4A. In contrast, there was no differ-
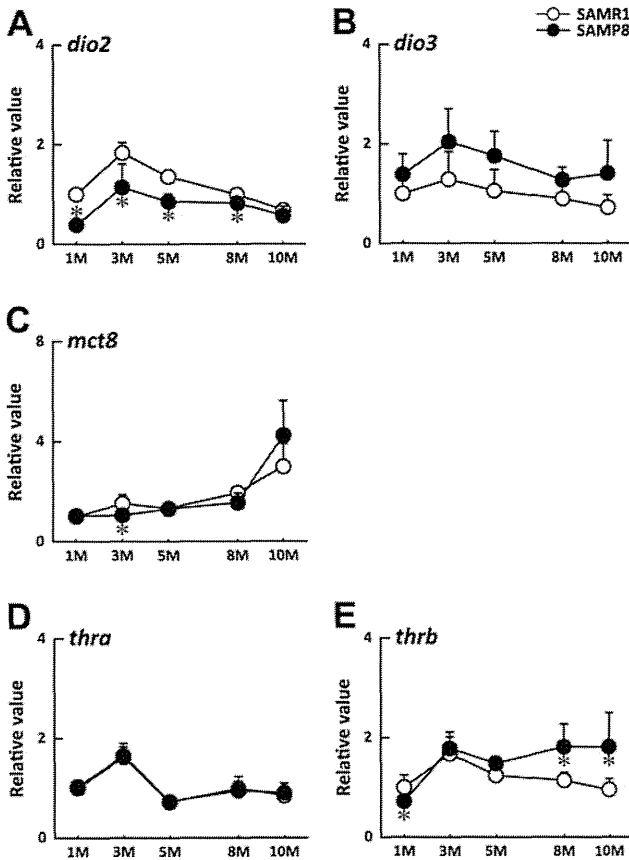
Fig. 3. Comparison of expression profiles of genes involved in TH metabolism and signaling in the hippocampus of SAMP8 and SAMR1. The mRNA expression of TH-metabolizing enzymes (**A:** *dio2*; **B:** *dio3*), a TH transporter (**C:** *mct8*), and TH receptors (**D:** *thra*; **E:** *thrb*) in the hippocampus of SAMP8 (solid circles) and SAMR1 (open circles) was quantified by real-time PCR at 1, 3, 5, 8, and 10 months using *ppia* as internal standard. Each mRNA level is expressed relative to that of SAMR1 at 1 month (means + SD of six mice/strain/age). *$P < 0.05$ between age-matched SAMP8 and SAMR1.

Fig. 4. D2 and D3 protein levels and D2 activity in the hippocampus of SAMP8 and SAMR1 at different ages. D2 (**A**) and D3 (**B**) protein levels quantified by Western blotting with anti-D2 and anti-D3 antibodies, respectively. Immunoreactive bands of D2 and D3 (examples shown in upper panels) in the hippocampus of SAMP8 (solid bars) and SAMR1 (open bars) at different ages were quantified using β-actin as standard and expressed relative to that of SAMR1 at 1 month. Results are expressed as means + SD [n = 6–8 (SAMR1), n = 5–6 (SAMP8)]. *$P < 0.05$ between age-matched SAMP8 vs. SAMR1. **C:** D2 enzyme activity in the hippocampus of SAMP8 (solid bars) and SAMR1 (open bars) at 1, 3, and 5 months expressed as means ± SD [n = 6 (SAMR1), n = 5–6 (SAMP8)]. *$P < 0.05$ between age-matched SAMP8 and SAMR1. #$P < 0.05$ compared with the value at 1 month of the same strain.

ence in D3 protein level between the two strains at all time points examined (Fig. 4B).

To compare further the D2 enzyme activity in the hippocampus of SAMR1 and SAMP8, iodothyronine deiodinase activity was first characterized with tissues from adult ICR mice. Hippocampal T4 deiodinating activity was not influenced by 1 mM PTU but was completely inhibited by 1 mM iopanoic acid. From the double reciprocal plot, kinetic constants for T4 were calculated to be $K_m = 4.7$ nM and $V_{max} = 68$ fmol I$^-$ released/mg protein/min. These characteristics of iodothyronine deiodinase activity were compatible with D2 activity.

In the SAMR1 hippocampus, D2 activity was highest at 1 month and significantly decreased (21–29%) with maturation of the animal at 3 and 5 months. Compared with that in SAMR1, hippocampal D2 activity was confirmed to be reduced by 21–23% in SAMP8 at 1, 3, and 5 months (Fig. 4C).
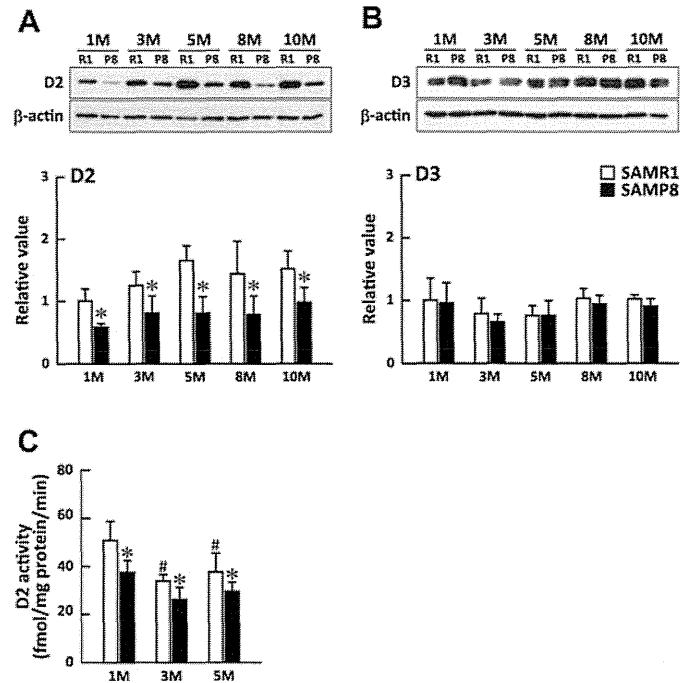
Differences in the Expression of TH-Responsive Genes in the Hippocampus of SAMP8 and SAMR1 Mice

To determine whether TH signaling was affected in the SAMP8 hippocampus as suggested by the reduction in the availability of active T3, we next examined the mRNA expression of the following four known TH-dependent genes; neurogranin (*rc3*), myelin basic protein (*mbp*), hairless (*hr*), and ectonucleotide pyrophosphatase/phosphodiesterase 2 (*enpp2*). These genes are either equipped with the TH-responsive element (TRE) or have a great possibility of possession of TRE (Farsetti et al., 1991; Martínez de Arrieta et al., 1999; Potter et al., 2002; Freitas et al., 2010). Although the mRNA expression of *rc3* was similar in both strains (Fig. 5A), expression of *hr* at 1, 3, 5, and 8 months and *mbp* at all time points and of *enpp2* at 3 months were significantly downregulated in the hippocampus of SAMP8 compared with SAMR1 (Fig. 5B–D).
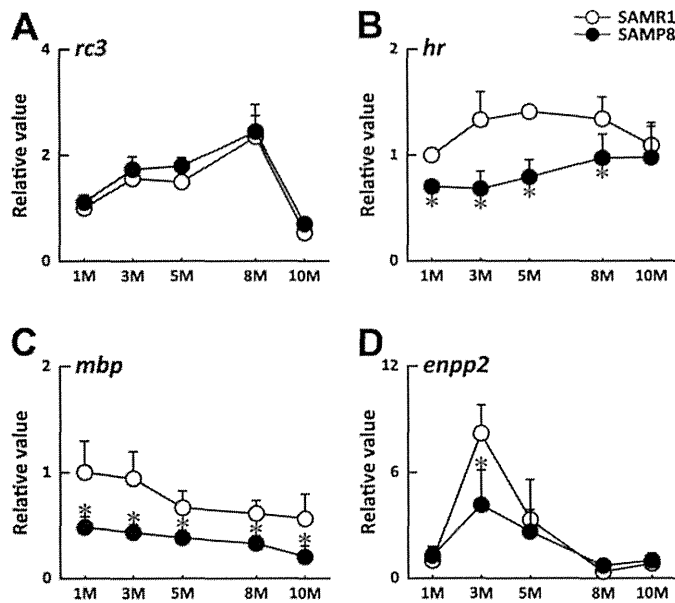
Fig. 5. Comparison of expression profiles of TH-responsive genes in the hippocampus of SAMP8 and SAMR1. The mRNA expression of rc3 (**A**), hr (**B**), mbp (**C**), and enpp2 (**D**) in the hippocampus of SAMP8 and SAMR1 was quantified by real-time PCR at 1, 3, 5, 8, and 10 months using ppia as internal standard. Each mRNA level is expressed relative to that of SAMR1 at 1 month (means + SD of six mice/strain/age). *$P < 0.05$ between age-matched SAMP8 and SAMR1.

Immunohistochemical Analysis of MBP Expression in the Hippocampus of SAMP8 and SAMR1 Mice

Because the mRNA expression of mbp in the SAMP8 hippocampus was significantly downregulated at all time points, we examined the expression of MBP protein by immunohistochemistry. As shown in Figure 6, prominent MBP immunoreactivity was observed in two regions of the hippocampus of both strains at all time points examined, one running along the stratum lacunosum-moleculare (open arrowheads in Fig. 6A) and the other running through the stratum radiatum of CA3 in a crescent shape (solid arrowheads in Fig. 6A). The former corresponds to the myelinated entorhinal projections (perforant path), and the latter corresponds mainly to the Schaffer collaterals, both of which are most intensively stained by other staining methods specific for myelin (Meier et al., 2004). The staining intensity appeared lower in SAMP8 compared with SAMR1 in these regions, especially at 1 month (Fig. 6A,B) and at 10 months (Fig. 6C,D). Quantification of total intensity of MBP immunoreactivity in two defined areas in the CA3 stratum radiatum (represented by squares a and b in Fig. 6E) at different time points showed a gradual increase in intensity up to 8 months in both strains (Fig. 6 F). Compared with that in SAMR1, MBP staining in SAMP8 was lower at 1, 3, and 8 months (Fig. 6F), suggesting a slower progression of myelination in the young SAMP8 mice, which never reached the

level of SAMR1 at its maximum (8 months). Furthermore, a significant reduction in MBP intensity observed only in SAMP8 at 10 months indicates an earlier onset of age-related myelin loss in SAMP8.

Distribution and Morphology of Astrocytes in the Hippocampus of SAMP8 and SAMR1

Because D2 is localized to astrocytes, we further examined whether a reduction in D2 protein and activity simply reflected a decrease in astrocyte population or not. By immunohistochemical staining of astrocytic cell bodies with S100β (Fig. 7A–D), the number density of astrocytes in the hippocampus of the two strains was found to be similar and constant between 1 month and 10 months (Fig. 7E). In contrast, the amount of GFAP was significantly increased in SAMP8 at 5, 8, and 10 months compared with SAMR1 (Fig. 7F), in accordance with the morphological changes into reactive astrocytes (data not shown) as reported previously for aged SAMP8 mice (Nomura et al., 1996).

DISCUSSION

Altered Local T3 Signaling in the Hippocampus of the Young SAMP8 Mouse

In the present study, we show for the first time significant alterations in the expression profiles of TH-metabolizing enzymes in the hippocampus of young SAMP8 compared with SAMR1. In SAMP8, large reductions in the dio2 mRNA level were observed between 1 month and 5 months, resulting in 35–50% reduction in the D2 protein level throughout the observation period (Figs. 3, 4) and significant reductions in D2 activity at 1 , 3, and 5 months (21–23%). On the other hand, D3 protein level was similar in both strains and was constant between 1 and 10 months.

Recent studies have established that TH signaling is precisely regulated locally by D2 and D3 activities (Dentice and Salvatore, 2011). The T3-degrading enzyme D3 is expressed mainly in fetal tissues, in which unoccupied TH receptors generally maintain cell proliferation and prevent premature differentiation (Williams, 2008). A rapid rise in T3 in mammals at birth is brought about by concomitant downregulation of dio3 and upregulation of dio2. Postnatal expression of dio3 is restricted to only a few tissues, including the brain, in which it is localized to neurons (Williams, 2008). Significant reduction in D2 protein and D2 activity with constant level of D3 protein observed in the present study thus suggests a decrease in the local availability of transcriptionally active T3 in the young SAMP8 hippocampus. Although it was not possible to assess the intracellular concentration of T3, weaker TH signaling in the SAMP8 hippocampus was confirmed by more than two-fold reductions in the expression of the three genes directly regulated by T3, especially at 3 and 5 months, when behavioral abnormalities of SAMP8 were most pronounced. Expression of one TH-responsive gene, RC3/neurogranin, was not altered in SAMP8,
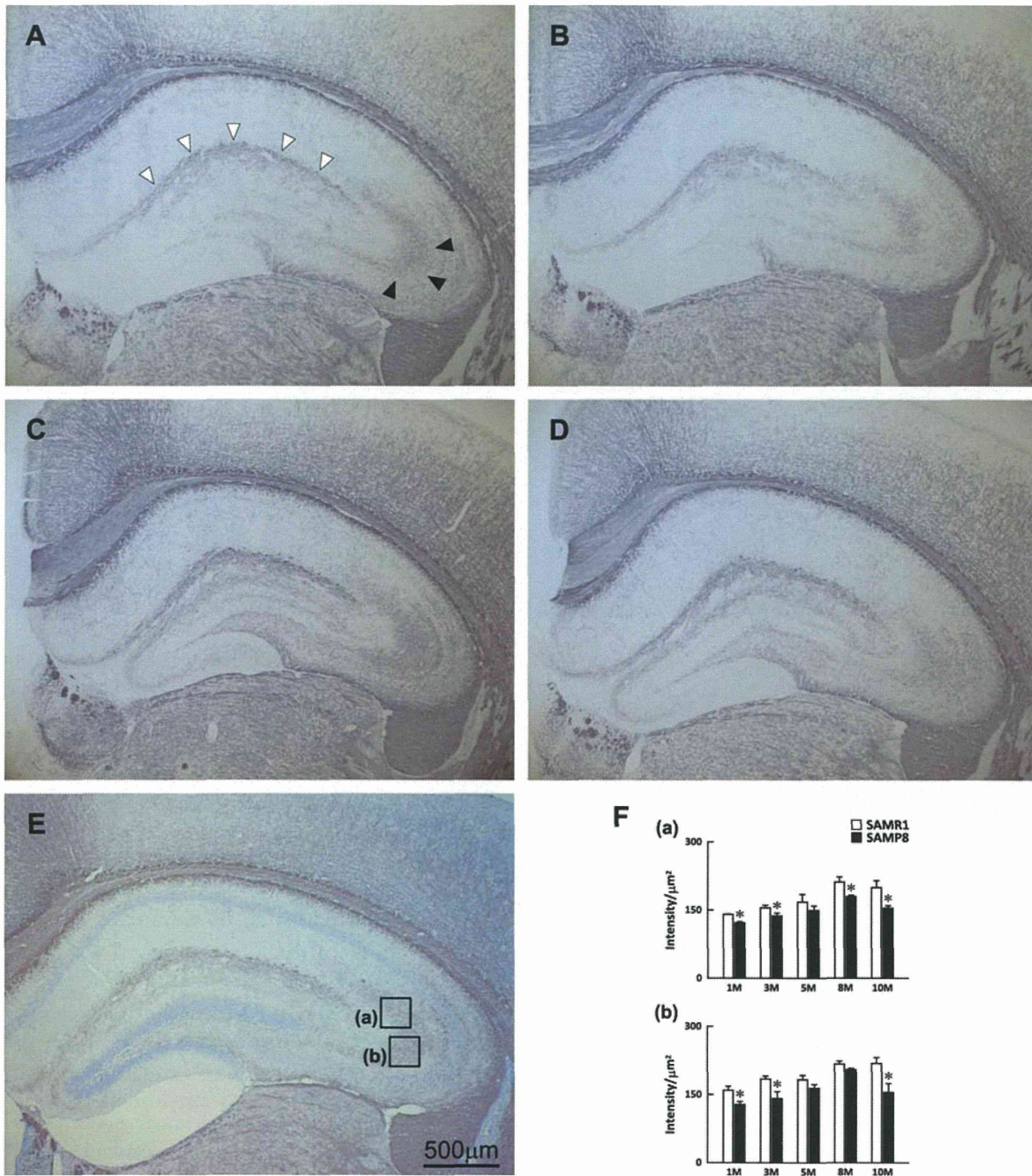
Fig. 6. Immunostaining with anti-MBP antibody in the hippocampus of SAMP8 and SAMR1 at different ages. Hippocampal sections (8 μm thick) from SAMP8 and SAMR1 aged 1, 3, 5, 8, and 10 months were stained with anti-MBP antibody. **A–D** show sections from SAMR1 (A) and SAMP8 (B) at 1 month and SAMR1 (C) and SAMP8 (D) at 10 months. Open arrowheads, stratum lacunosum-moleculare; solid arrowheads, stratum radiatum of CA3. In **E**, a section from SAMR1 at 5 months counterstained with hematoxylin is shown. **F:** Total intensity of MBP immunoreactivity in two defined areas in CA3 (represented by the two squares in E) was quantified individually at different time points. Results are expressed as means + SD. Three sections per mouse and three mice/strain/age were analyzed. *$P < 0.05$ between age-matched SAMP8 and SAMR1.

probably because this gene for the postsynaptic protein is abundantly expressed only between 1 and 2 weeks postnatally.

Further studies are needed to determine the causes of the reduction of D2 protein and D2 activity in SAMP8 mice. D2 is an endoplasmic reticulum
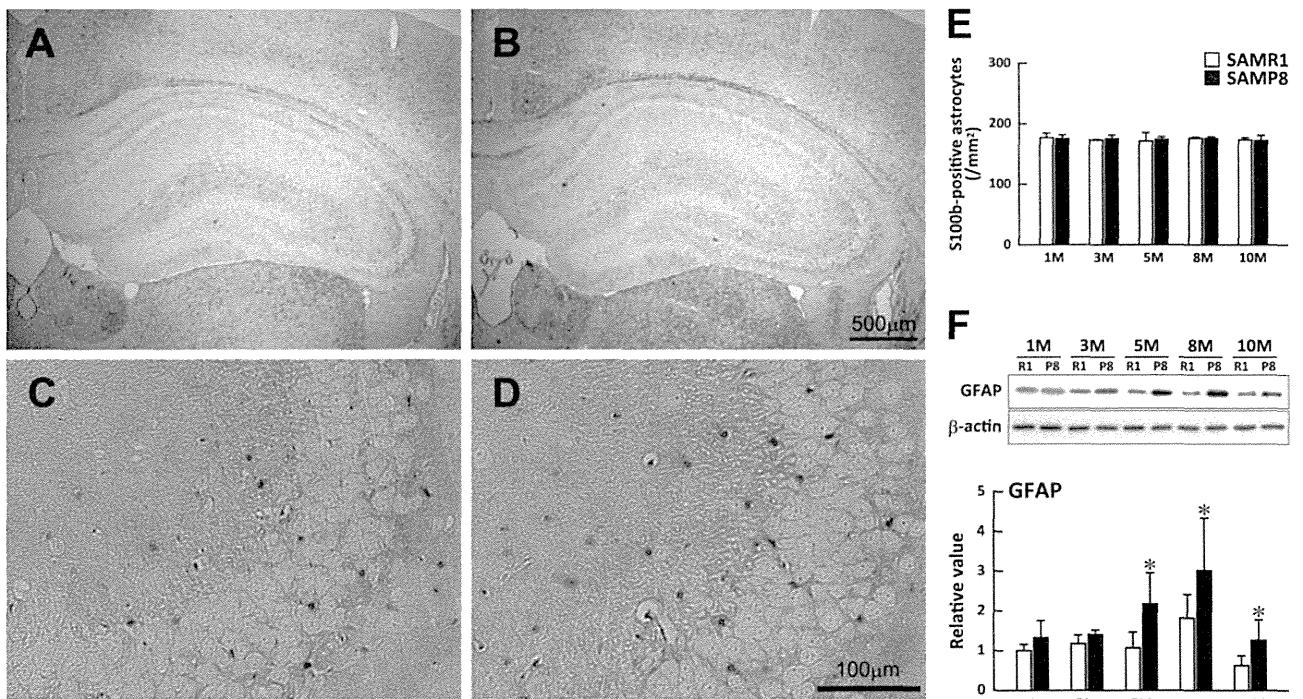
Fig. 7. Astrocyte density and GFAP content of the SAMP8 and SAMR1 hippocampus at different ages. Astrocyte cell bodies were visualized by immunostaining with anti-S100B antibody in the whole hippocampus (**A,B**) and CA3 region (**C,D**) of SAMR1 (A,C) and SAMP8 (B,D) mice at 3 months. **E:** Number densities of astrocytes in the whole hippocampus of SAMR1 (open bars) and SAMP8 (solid bars) were obtained by counting S100B-positive cell bodies at different ages and expressed as mean + SD [n = 3–8 (SAMR1, SAMP8)].

F: GFAP content of the SAMR1 (open bars) and SAMP8 (solid bars) hippocampus quantified by Western blotting with anti-GFAP antibody. Immunoreactive bands of GFAP (examples shown in the upper panel) at different ages were quantified using β-actin as standard and expressed relative to that of SAMR1 at 1 month. Results are expressed as means + SD [n = 5–8 (SAMR1), n = 5–6 (SAMP8)]. *$P < 0.05$ between age-matched SAMP8 and SAMR1.

(ER)-resident protein in astrocytes and tanycytes regulated posttranslationally by ubiquitination-dependent inactivation and degradation, which are enhanced by T4 (for review see Arrojo e Drigo and Bianco, 2011). Because the densities of S100B-positive astrocytes were similar and constant with age in both strains and GFAP immunoreactivity in the SAMP8 hippocampus was comparable to that in SAMR1 up to 3 months (Fig. 7), we can rule out the possibility that the reduction in D2 protein simply reflects a decrease in astrocyte population. At the transcriptional level, *dio2* has been shown to be downregulated by oxidative stress and inflammation, whereas *dio3* is upregulated (Lamirand et al., 2008; Simonides et al., 2008; Calzà et al., 2010). Such reciprocal changes in the expression of *dio2* and *dio3* in response to pathological conditions lead to reduced local T3 concentration, which in turn should decrease metabolic activity and prevent further production of oxidative stress. Reduced expression of *dio2* in SAMP8 at older ages may arise from elevated oxidative stress (Butterfield et al., 1997; Tomobe et al., 2012) or chronic expression of proinflammatory cytokines such as interleukin (IL)-1β, IL-6, and tumor necrosis factor-α (Tha et al., 2000) reported for SAMP8 at 10 months. On the other hand, an explanation for the severe downregulation of *dio2* at

earlier time points (1 and 3 months) awaits further studies on the perinatal development of the TH system of SAMP8.

Delayed Myelination Followed by Earlier Onset of Myelin Degeneration in the SAMP8 Hippocampus

In addition to signs of oxidative stress (Butterfield et al., 1997) and increased amyloid β burden (Del Valle et al., 2010), loss of myelin and myelinating oligodendrocytes have been previously reported for the brains of old SAMP8 (10 months of age; Tanaka et al., 2005). The present study reveals that there is already an impairment of myelination during development.

It is well established that TH plays a critical role in developmental myelination, both through regulation of oligodendrocyte differentiation and through expression of myelin component genes such as *mbp* (Oppenheimer and Schwartz, 1997; Koibuchi and Chin, 2000). Importance of TH in remyelination in the adult CNS has also been highlighted in recent studies on inflammatory-demyelinating diseases in which immune activation and brain injury downregulate *dio2* and lead to a decrease in local T3 availability (Calzà et al., 2005, 2010). A decrease in MBP immunoreactivity observed in SAMP8

at later time points (10 months) may result from downregulation of *dio2* by oxidative stress and/or by proinflammatory cytokines.

Possible Relationship Between TH Deficiency and Abnormal Behavior of Young SAMP8 Mice

In addition to the age-associated cognitive impairment, behavioral abnormalities of SAMP8 mice have been described in an earlier study by Miyamoto et al. (1992), in which the authors detected lower anxiety in an elevated plus maze test, food neophobia, and punished drinking test. These behavioral characteristics were noted at 4 months in SAMP8 and became progressively more pronounced with age. Because a reduction in anxiety was also found in SAMR1 at a much older age (20 months), it was concluded that behavioral abnormalities of SAMP8 was an earlier manifestation of age-related emotional disorders. By comparing SAMP8 and SAMR1 at 4 months and 15 months, Markowska et al. (1998) also noted reduced anxiety by plus maze test, hyperactivity by open-field test, and an age-related impairment of sensorimotor performance.

Our study on the behavior of the two strains at five time points between 1 month and 10 months clearly demonstrated that hyperactivity and reduced anxiety were not aging-dependent behavioral abnormalities but were characteristic of young SAMP8 before the onset of cognitive decline. Reduced TH signaling resulting from downregulation of *dio2* overlaps in timing with behavioral alterations, suggesting a possible link between the two phenomena.

Two lines of evidence relate the developmental deficiency in TH signaling to attention deficit-hyperactivity disorder (ADHD) in humans. One is the high incidence of ADHD (40–70%) associated with generalized resistance to thyroid hormone (RTH), a rare genetic syndrome caused by mutations in the TH receptor β (TRβ) gene that result in reduced T3 binding (Hauser et al., 1993). RTH is characterized by elevated serum T4 and T3 concentrations, accompanied by normal or elevated level of thyroid-stimulating hormone (TSH) and by reduced responsiveness of the pituitary and peripheral tissues to TH. Knock-in mice expressing a human mutant TRβ allele (TRβPV) found in RTH exhibited hyperactivity, impaired learning, and altered responsiveness to methylphenidate resembling human ADHD (Siesser et al., 2005, 2006).

The second piece of evidence linking TH and ADHD comes from studies on preterm infants (Simic et al., 2009). Because the fetal thyroid does not produce significant amounts of TH until the third trimester in humans (Williams, 2008), most preterm infants experience a transient neonatal hypothyroidism during what should have been the later part of pregnancy in which maternal TH supply is still important. TH insufficiency is thus considered a major cause of neurocognitive deficits with reduced attention at 3 months of age (Simic et al., 2009). Attention-deficit and hyperactive behavior

could also be reproduced in an animal model of perinatal hypothyroidism obtained by administering PTU to pregnant rats during pregnancy and lactation periods (Negishi et al., 2005). Although body weights at birth were comparable to those of euthyroid pups, offspring of PTU-treated dams showed a reduction in postnatal body weight increase. When tested behaviorally at the young adult stage (8 weeks of age), they exhibited hyperactivity, low anxiety, impaired learning, and shortened attention span compared with euthyroid animals.

Although SAMP8 mice have been considered as models of age-dependent cognitive disorders, our study shows that, at younger ages, they may serve as an interesting model of developmental disorders caused by local T3 deficiency. The present results also raise the possibility that accelerated senescence in SAMP8 mice may originate from subclinical deficits in TH signaling during development. Perturbations in the TH system can occur not only endogenously but also through environmental factors such as iodine or Se deficiency and intake of some chemicals (Takahashi et al., 2009), so studies on SAMP8 both at younger and at older ages should provide valuable insights into the role of the TH system in the development and maintenance of the CNS.

REFERENCES

Arrojo e Drigo R, Bianco AC. 2011. Type 2 deiodinase at the crossroads of thyroid hormone action. Int J Biochem Cell Biol 43:1432–1441.

Bernal J. 2005. Thyroid hormones and brain development. Vitam Horm 71:95–122.

Bradford MM. 1976. A rapid and sensitive method for the quantitation of microgram quantities of protein utilizing the principle of protein-dye binding. Anal Biochem 72:248–254.

Butterfield DA, Poon HF. 2005. The senescence-accelerated prone mouse (SAMP8): a model of age-related cognitive decline with relevance to alterations of the gene expression and protein abnormalities in Alzheimer's disease. Exp Gerontol 40:774–783.

Butterfield DA, Howard BJ, Yatin S, Allen KL, Carney JM. 1997. Free radical oxidation of brain proteins in accelerated senescence and its modulation by N-tert-butyl-alpha-phenylnitrone. Proc Natl Acad Sci U S A 94:674–678.

Calzà L, Fernandez M, Giuliani A, D'Intino G, Pirondi S, Sivilia S, Paradisi M, Desordi N, Giardino L. 2005. Thyroid hormone and remyelination in adult central nervous system: a lesson from an inflammatory-demyelinating disease. Brain Res Rev 48:339–346.

Calzà L, Fernandez M, Giardino L. 2010. Cellular approaches to central nervous system remyelination stimulation: thyroid hormone to promote myelin repair via endogenous stem and precursor cells. J Mol Endocrinol 44:13–23.

Colas D, Cespuglio R, Sarda N. 2005. Sleep wake profile and EEG spectral power in young or old senescence accelerated mice. Neurobiol Aging 26:265–273.

Davis JD, Tremont G. 2007. Neuropsychiatric aspects of hypothyroidism and treatment reversibility. Minerva Endocrinol 32:49–65.

Del Valle J, Duran-Vilaregut J, Manich G, Casadesús G, Smith MA, Camins A, Pallàs M, Pelegrí C, Vilaplana J. 2010. Early amyloid

accumulation in the hippocampus of SAMP8 mice. J Alzheimers Dis 19:1303–1315.

Dentice M, Salvatore D. 2011. Deiodinases: the balance of thyroid hormone: local impact of thyroid hormone inactivation. J Endocrinol 209:273–282.

Farsetti A, Mitsuhashi T, Desvergne B, Robbins J, Nikodem VM. 1991. Molecular basis of thyroid hormone regulation of myelin basic protein gene expression in rodent brain. J Biol Chem 266:23226–23232.

Flood JF, Morley JE. 1992. Early onset of age-related impairment of aversive and appetitive learning in the SAM-P/8 mouse. J Gerontol 47:B52–B59.

Flood JF, Morley JE. 1993. Age-related changes in footshock avoidance acquisition and retention in senescence accelerated mouse (SAM). Neurobiol Aging 14:153–157.

Freitas BC, Gereben B, Castillo M, Kalló I, Zeöld A, Egri P, Liposits Z, Zavacki AM, Maciel RM, Jo S, Singru P, Sanchez E, Lechan RM, Bianco AC. 2010. Paracrine signaling by glial cell-derived triiodothyronine activates neuronal gene expression in the rodent brain and human cells. J Clin Invest 120:2206–2217.

Gereben B, Zavacki AM, Ribich S, Kim BW, Huang SA, Simonides WS, Zeöld A, Bianco AC. 2008. Cellular and molecular basis of deiodinase-regulated thyroid hormone signaling. Endocr Rev 29:898–938.

Hauser P, Zametkin AJ, Martinez P, Vitiello B, Matochik JA, Mixson AJ, Weintraub BD. 1993. Attention deficit-hyperactivity disorder in people with generalized resistance to thyroid hormone. N Engl J Med 328:997–1001.

Koibuchi N, Chin WW. 2000. Thyroid hormone action and brain development. Trends Endocrinol Metab 11:123–128.

Lamirand A, Pallud-Mothré S, Ramaugé M, Pierre M, Courtin F. 2008. Oxidative stress regulates type 3 deiodinase and type 2 deiodinase in cultured rat astrocytes. Endocrinology 149:3713–3721.

Markowska AL, Spangler EL, Ingram DK. 1998. Behavioral assessment of the senescence-accelerated mouse (SAM P8 and R1). Physiol Behav 64:15–26.

Martínez de Arrieta C, Morte B, Coloma A, Bernal J. 1999. The human RC3 gene homolog, NRGN contains a thyroid hormone-responsive element located in the first intron. Endocrinology 140:335–343.

Meier S, Bräuer AU, Heimrich B, Nitsch R, Savaskan NE. 2004. Myelination in the hippocampus during development and following lesion. Cell Mol Life Sci 61:1082–1094.

Miyamoto M, Kiyota Y, Yamazaki N, Nagaoka A, Matsuo T, Nagawa Y, Takeda T. 1986. Age-related changes in learning and memory in the senescence-accelerated mouse (SAM). Physiol Behav 38:399–406.

Miyamoto M, Kiyota Y, Nishiyama M, Nagaoka A. 1992. Senescence-accelerated mouse (SAM): age-related reduced anxiety-like behavior in the SAM-P/8 strain. Physiol Behav 51:979–985.

Murakami M, Tanaka K, Greer MA, Mori M. 1988. Anterior pituitary type II thyroxine 5′-deiodinase activity is not affected by lesions of the hypothalamic paraventricular nucleus which profoundly depress pituitary thyrotropin secretion. Endocrinology 123:1676–1681.

Negishi T, Kawasaki K, Sekiguchi S, Ishii Y, Kyuwa S, Kuroda Y, Yoshikawa Y. 2005. Attention-deficit and hyperactive neurobehavioural characteristics induced by perinatal hypothyroidism in rats. Behav Brain Res 159:323–331.

Nomura Y, Yamanaka Y, Kitamura Y, Arima T, Ohnuki T, Oomura Y, Sasaki K, Nagashima K, Ihara Y. 1996. Senescence-accelerated mouse. Neurochemical studies on aging. Ann N Y Acad Sci 786:410–418.

Oppenheimer JH, Schwartz HL. 1997. Molecular basis of thyroid hormone-dependent brain development. Endocr Rev 18:462–475.

Potter GB, Zarach JM, Sisk JM, Thompson CC. 2002. The thyroid hormone-regulated corepressor hairless associates with histone deacetylases in neonatal rat brain. Mol Endocrinol 16:2547–2560.

Siesser WB, Cheng SY, McDonald MP. 2005. Hyperactivity, impaired learning on a vigilance task, and a differential response to methylphenidate in the TRbetaPV knock-in mouse. Psychopharmacology 181:653–663.

Siesser WB, Zhao J, Miller LR, Cheng SY, McDonald MP. 2006. Transgenic mice expressing a human mutant beta1 thyroid receptor are hyperactive, impulsive, and inattentive. Genes Brain Behav 5:282–297.

Simic N, Asztalos EV, Rovet J. 2009. Impact of neonatal thyroid hormone insufficiency and medical morbidity on infant neurodevelopment and attention following preterm birth. Thyroid 19:395–401.

Simonides WS, Mulcahey MA, Redout EM, Muller A, Zuidwijk MJ, Visser TJ, Wassen FW, Crescenzi A, da-Silva WS, Harney J, Engel FB, Obregon MJ, Larsen PR, Bianco AC, Huang SA. 2008. Hypoxia-inducible factor induces local thyroid hormone inactivation during hypoxic-ischemic disease in rats. J Clin Invest 118:975–983.

Takahashi M, Negishi T, Tashiro T. 2008. Identification of genes mediating thyroid hormone action in the developing mouse cerebellum. J Neurochem 104:640–652.

Takahashi M, Negishi T, Imamura M, Sawano E, Kuroda Y, Yoshikawa Y, Tashiro T. 2009. Alterations in gene expression of glutamate receptors and exocytosis-related factors by a hydroxylated-polychlorinated biphenyl in the developing rat brain. Toxicology 257:17–24.

Takeda T. 2009. Senescence-accelerated mouse (SAM) with special references to neurodegeneration models, SAMP8 and SAMP10 mice. Neurochem Res 34:639–659.

Takeda T, Hosokawa M, Takeshita S, Irino M, Higuchi K, Matsushita T, Tomita Y, Yasuhira K, Hamamoto H, Shimizu K, Ishii M, Yamamuro T. 1981. A new murine model of accelerated senescence. Mech Aging Dev 17:183–194.

Tanaka J, Okuma Y, Tomobe K, Nomura Y. 2005. The age-related degeneration of oligodendrocytes in the hippocampus of the senescence-accelerated mouse (SAM) P8: a quantitative immunohistochemical study. Biol Pharm Bull 28:615–618.

Tha KK, Okuma Y, Miyazaki H, Murayama T, Uehara T, Hatakeyama R, Hayashi Y, Nomura Y. 2000. Changes in expressions of proinflammatory cytokines IL-1beta, TNF-alpha and IL-6 in the brain of senescence-accelerated mouse (SAM) P8. Brain Res 885:25–31.

Tomobe K, Nomura Y. 2009. Neurochemistry, neuropathology, and heredity in SAMP8: a mouse model of senescence. Neurochem Res 34:660–669.

Tomobe K, Shinozuka T, Kuroiwa M, Nomura Y. 2012. Age-related changes of Nrf2 and phosphorylated GSK-3β in a mouse model of accelerated aging (SAMP8). Arch Gerontol Geriatr 54:e1–e7.

Williams GR. 2008. Neurodevelopmental and neurophysiological actions of thyroid hormone. J Neuroendocrinol 20:784–794.

Yagi H, Katoh S, Akiguchi I, Takeda T. 1988. Age-related deterioration of ability of acquisition in memory and learning in senescence accelerated mouse: SAM-P/8 as an animal model of disturbances in recent memory. Brain Res 474:86–93.

Original article

Prenatal exposure to organomercury, thimerosal, persistently impairs the serotonergic and dopaminergic systems in the rat brain: Implications for association with developmental disorders

Michiru Ida-Eto [a,*], Akiko Oyabu [a], Takeshi Ohkawara [a], Yasura Tashiro [a], Naoko Narita [b], Masaaki Narita [a]

[a] Department of Anatomy II, Mie University Graduate School of Medicine, Tsu, Mie 514-8507, Japan
[b] Department of Education, Bunkyo University, Koshigaya, Saitama 343-8511, Japan

Abstract

Thimerosal, an organomercury compound, has been widely used as a preservative. Therefore, concerns have been raised about its neurotoxicity. We recently demonstrated perturbation of early serotonergic development by prenatal exposure to thimerosal (Ida-Eto et al. (2011) [11]). Here, we investigated whether prenatal thimerosal exposure causes persistent impairment after birth. Analysis on postnatal day 50 showed significant increase in hippocampal serotonin following thimerosal administration on embryonic day 9. Furthermore, not only serotonin, striatal dopamine was significantly increased. These results indicate that embryonic exposure to thimerosal produces lasting impairment of brain monoaminergic system, and thus every effort should be made to avoid the use of thimerosal.
© 2012 The Japanese Society of Child Neurology. Published by Elsevier B.V. All rights reserved.

Keywords: Thimerosal; Serotonin; Dopamine; Embryonic exposure; Developmental disorders; Rat

1. Introduction

Thimerosal, an organomercury compound, has been widely used as a preservative [1]. Thimerosal is metabolized first to ethylmercury and further to inorganic mercury, both of which accumulate in the brain and other organs and have neurotoxic activity [2,3]. Accordingly, use of thimerosal such as vaccines is of great concern, particularly on infants and fetuses [4,5], and therefore, efforts have been made to reduce thimerosal from vaccines [6].

The adverse effects of thimerosal after neonatal administration include impaired pain sensitivity [7],

hippocampal neurodegeneration [8], and changes in the dopamine system with subsequent behavioral disorders [9]. In addition, thimerosal was shown to affect neurite extension of neuroblastoma cells in vitro, therefore, it is evident that thimerosal leads to neurological abnormalities [10]. However, little is known regarding the prenatal effects of thimerosal. We recently reported that exposure of pregnant rats at gestational day 9 (E9) to thimerosal increased the number of serotonergic neurons in the lateral portion of the caudal raphe in E15 rat hindbrain and thus prenatal thimerosal exposure impaired early serotonergic development [11]. We have also demonstrated that prenatal exposure at E9 to thalidomide or valproic acid (VPA) specifically caused long-term effects on the normal development of serotonergic neuronal systems [12,13], accompanied with behavioral abnormalities that mimicked human

* Corresponding author. Address: Department of Anatomy II, Mie University Graduate School of Medicine, 2-174 Edobashi, Tsu, Mie 514-8507, Japan. Tel.: +81 59 232 1111x6326; fax: +81 59 232 8031.
E-mail address: etom@doc.medic.mie-u.ac.jp (M. Ida-Eto).

autism [14]. Although a relationship between autism and thimerosal has not been confirmed yet [15,16], we need to know whether prenatal thimerosal exposure effects can persist into adulthood. Here, we investigated serotonin and dopamine content in the brains of postnatal day 50 (P50) adult rats following prenatal treatment of thimerosal.

2. Materials and methods

Pregnant Wistar rats were purchased from CLEA Japan, Inc. (Tokyo, Japan). Thimerosal (Sigma–Aldrich, St. Louis, MO) was dissolved in saline, and was administered to pregnant rats on E9 in volume of 50 μl by intramuscular injection into the *glutei maximi*. Thimerosal doses per injection were: 1, 0.1 and 0.01 mg Hg/kg. For the control group, saline was administered in the same manner. Three dams for each group were examined. All animal experiments were authorized by the Animal Research Committee of Mie University.

Measurement of concentration of serotonin (5-HT), dopamine (DA) and their metabolites 5-hydroxyindoleacetic acid (5-HIAA), 3,4-dihydroxyphenylacetic acid (DOPAC) and homovanillic acid (HVA) were performed as described previously [12]. Because brain 5-HT levels are influenced by estrus cycle in females, we used the tissues only from male animals. Each offspring was deeply anesthetized on P50 and then decapitated. The hippocampus and striatum were immediately removed on ice, collected into a tube, frozen with liquid nitrogen, and stored at −80 °C until assay. The tissues were homogenized using an ultrasonic homogenizer (NR-50M; Microtec, Chiba, Japan) in 5 volumes of a mixture of 0.2 M perchloric acid, 100 μM EDTA, and 200 ng of isoproterenol hydrochloride as an internal standard and incubated on ice for 30 min. After centrifugation (20,000g, 20 min, 4 °C), the supernatant was adjusted to pH 3 with 1 M sodium acetate and filtered through a 0.45-μm pore size membrane filter (Millex-LH; Millipore, Billerica, MA). A part of the aliquot was separated by high performance liquid chromatography (HPLC) with an electrochemical detector (HTEC-500; Eicom, Kyoto, Japan) and an Eicompak SC-5 ODS column (3.0 mm × 150 mm, Eicom). The mobile phase (0.1 M sodium acetate–citrate acid buffer, pH 3.5, 17% methanol, 190 mg/L sodium 1-octanesulfonate, and 5 mg/L EDTA) allowed for the separation of 5-HT and DA, and their metabolites. Consistent results were obtained from three independent experiments. Statistical evaluation was carried out by grouped t-test.

3. Results

To evaluate the potential effects of embryonic exposure to thimerosal on postnatal brain monoamine content, different doses of thimerosal (1, 0.1, and

0.01 mg Hg/kg) were administered to E9 pregnant rats, and then allowed to have pups. When exposed to 1 mg Hg/kg thimerosal, most of the pups were dead soon after birth. On the other hand, in the 0.1 and 0.01 mg Hg/kg thimerosal-exposed groups, no major anomalies, growth retardation, or reduced number of delivered pups were observed in the two groups. Therefore, for monoamine content analysis, thimerosal doses of 0.1 and 0.01 mg Hg/kg were used. Concentrations of hippocampal 5-HT and striatal DA on P50 were measured by HPLC. As shown in the Fig. 1, a significant increase in hippocampal 5-HT levels was observed in the thimerosal-exposed groups (0.01 mg Hg/kg, 266.2 ± 22.2 ng/g weight, $p < 0.05$ vs. control; 0.1 mg Hg/kg, 307.0 ± 7.2 ng/g weight, $p < 0.01$ vs. control; control group, 177.8 ± 27.8 ng/g weight). Striatal DA concentrations were also significantly increased in the exposed groups (0.01 mg Hg/kg, 7039 ± 448 ng/g weight,

(A) hippocampal serotonin
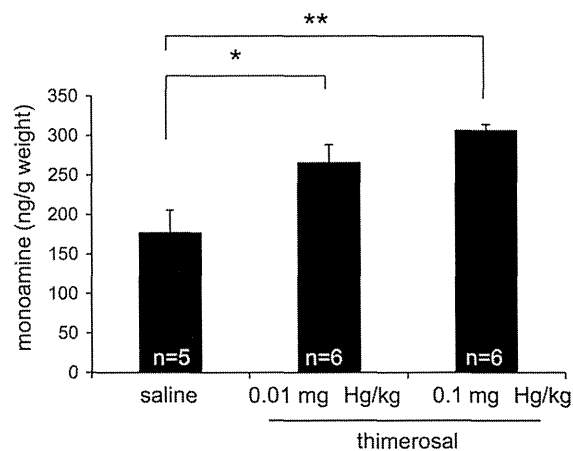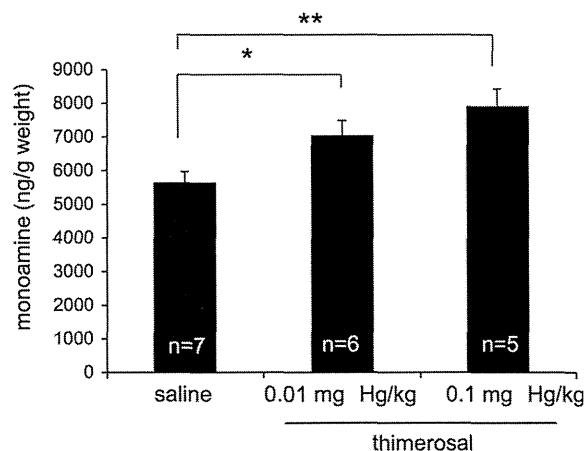

(B) striatal dopamine

Fig. 1. Monoamine levels in control vs. thimerosal-exposed rats (ng/g weight). Different doses of thimerosal (0.1, and 0.01 mgHg/kg) were administered to E9 pregnant rats, and then allowed to have pups. On P50, concentrations of hippocampal serotonin and striatal dopamine were measured by HPLC. Values are mean ± SEM. $^*p < 0.05$ vs. control; $^{**}p < 0.01$ vs. control.

$p < 0.05$ vs. control; 0.1 mg Hg/kg, 7905 ± 520 ng/g weight, $p < 0.01$ vs. control; control group, 5643 ± 323 ng/g weight). Hippocampal 5-HIAA, a metabolite of 5-HT, was also increased in thimerosal-exposed groups compared to control (0.01 mg Hg/kg, 457.8 ± 30.8 ng/g weight, not significant to control; 0.1 mg Hg/kg, 477.4 ± 20.2 ng/g weight, $p < 0.05$ vs. control; control group, 388.2 ± 35.3 ng/g weight), but its increase was not as much as that of 5-HT. Subsequently, the ratio 5-HIAA/5-HT was decreased (control, 2.32 ± 0.26; 0.01 mg Hg/kg, 1.75 ± 0.11, $p < 0.05$ vs. control; 0.1 mg Hg/kg, 1.56 ± 0.06, $p < 0.01$ vs. control). Striatal DOPAC and HVA, a metabolite of DA, was not changed statistically in thimerosal-exposed groups compared to control (0.01 mg Hg/kg, 2082 ± 152 ng/g weight, not significant to control; 0.1 mg Hg/kg, 2225 ± 100 ng/g weight, not significant to control; control group, 1997 ± 103 ng/g weight). The ratio (DOPAC + HVA)/DA was also decreased (control, 0.356 ± 0.011; 0.01 mg Hg/kg, 0.295 ± 0.007, $p < 0.01$ vs. control; 0.1 mg Hg/kg, 0.283 ± 0.010, $p < 0.01$ vs. control). These results indicate that prenatal exposure to thimerosal on E9 affects levels of 5-HT and DA, and their metabolites in the adult brain.

4. Discussion

In this study, we demonstrated that prenatal exposure to thimerosal on E9 caused a significant increase in 5-HT and DA content in the brains of adult rats. This finding indicates that prenatal thimerosal exposure may cause lasting neurochemical impairments to the serotonergic and dopaminergic systems.

Prenatal exposure to thimerosal has been shown to alter early embryonic development of 5-HT in our previous study [11]. These findings, together with those of the present study, suggest that a single prenatal exposure to thimerosal causes irreversible and critical effects to the brain serotonergic system. Persistent effects caused by a single prenatal exposure to chemicals are not, however, surprising because we have previously reported that prenatal exposure on E9 to thalidomide or VPA, chemicals known to induce autism when exposed at E9 [17,18], also induced increased hippocampal 5-HT in the adult brains of rats at P50 [12,13]. In thalidomide or VPA experiments, behavioral abnormalities in rats closely mimicked human autism [14]. Importantly, we also showed that abnormalities in 5-HT content caused by prenatal thalidomide exposure were time-specific (i.e., on E9). Therefore, the present result that exposure to thimerosal on E9 caused 5-HT abnormalities is consistent with previous findings. Because the possible link between thimerosal and autism is still controversial [15,16], further experiments are necessary to resolve this issue.

Prenatal exposure to thimerosal also seems to cause persistent changes in the striatal dopaminergic neuron of the brain. Faro et al. demonstrated that ethylmercury and methylmercury increased the *in vivo* release of DA from the striatum in free-moving adult rats [19]. Olczak et al. demonstrated that early postnatal administration of thimerosal caused persistent changes of the dopamine system in rats [9]. Therefore, mercury can cause short- and long-term effects on the dopaminergic system. However, to the best of our knowledge, our present report is the first to demonstrate that the effects from prenatal exposure to thimerosal persisted through the P50 dopaminergic and serotonergic systems. Because both dopaminergic and serotonergic neurons are known to be fated to develop from precursors starting from about E9, with help from the sonic hedgehog and fibroblast growth factor 8 genes [20], exposure to thimerosal at E9 is thought to cause irreversible effects on serotonergic and dopaminergic neurons. Further experiments are necessary to determine how thimerosal perturbs the normal development of both neurons.

Hippocampal 5-HIAA, a metabolite of 5-HT, were also increased in thimerosal-exposed groups compared to control, but its increase was not as much as that of 5-HT. Subsequently, the ratio 5-HIAA/5-HT was apparently decreased. Striatal (DOPAC + HVA)/DA ratio was decreased. We are not sure whether this decreased ratio means the true change of neurotransmitter metabolism, i.e., change of monoamine oxidase (MAO) level. However, in any case, the fact that thimerosal-dependent increase of 5-HT was more or less accompanied by 5-HIAA increase and that thimerosal-dependent increase of DA suggests that fetal exposure to thimerosal causes somehow lasting change of neurotransmitter metabolism. Further study to lead the conclusion of the effects of thimerosal on neurotransmitter metabolism such as by analyzing MAO activity will be published elsewhere.

Acknowledgment

References

[1] Magos L. Review on the toxicity of ethylmercury, including its presence as a preservative in biological and pharmaceutical products. J Appl Toxicol 2001;21:1–5.
[2] Clarkson TW, Magos L. The toxicology of mercury and its chemical compounds. Crit Rev Toxicol 2006;36:609–62.
[3] Dórea JG. Integrating experimental (*in vitro* and *in vivo*) neurotoxicity studies of low-dose thimerosal relevant to vaccines. Neurochem Res 2011;36:927–38.

[4] Ball LK, Ball R, Pratt RD. An assessment of thimerosal use in childhood vaccines. Pediatrics 2001;107:1147–54.

[5] Young HA, Geier DA, Geier MR. Thimerosal exposure in infants and neurodevelopmental disorders: an assessment of computerized medical records in the Vaccine Safety Datalink. J Neurol Sci 2008;271:110–8.

[6] Verstraeten T, Davis RL, DeStefano F, Lieu TA, Rhodes PH, Black SB, et al. Safety of thimerosal-containing vaccines: a two-phased study of computerized health maintenance organization databases. Pediatrics 2003;112:1039–48.

[7] Olczak M, Duszczyk M, Mierzejewski P, Majewska MD. Neonatal administration of a vaccine preservative, thimerosal, produces lasting impairment of nociception and apparent activation of opioid system in rats. Brain Res 2009;1301:143–51.

[8] Olczak M, Duszczyk M, Mierzejewski P, Bobrowicz T, Majewska MD. Neonatal administration of thimerosal causes persistent changes in mu opioid receptors in the rat brain. Neurochem Res 2010;35:1840–7.

[9] Olczak M, Duszczyk M, Mierzejewski P, Meyza K, Majewska MD. Persistent behavioral impairments and alterations of brain dopamine system after early postnatal administration of thimerosal in rats. Behav Brain Res 2011;223:107–18.

[10] Lawton M, Iqbal M, Kontovraki M, Lloyd Mills C, Hargreaves AJ. Reduced tubulin tyrosination as an early marker of mercury toxicity in differentiating N2a cells. Toxicol In Vitro 2007;21:1258–61.

[11] Ida-Eto M, Oyabu A, Ohkawara T, Tashiro Y, Narita N, Narita M. Embryonic exposure to thimerosal, an organomercury compound, causes abnormal early development of serotonergic neurons. Neurosci Lett 2011;505:61–4.

[12] Narita N, Kato M, Tazoe M, Miyazaki K, Narita M, Okado N. Increased monoamine concentration in the brain and blood of fetal thalidomide- and valproic acid-exposed rat: putative animal models for autism. Pediatr Res 2002;52:576–9.

[13] Miyazaki K, Narita N, Narita M. Maternal administration of thalidomide or valproic acid causes abnormal serotonergic neurons in the offspring: implication for pathogenesis of autism. Int J Dev Neurosci 2005;23:287–97.

[14] Narita M, Oyabu A, Imura Y, Kamada N, Yokoyama T, Tano K, et al. Nonexploratory movement and behavioral alterations in a thalidomide or valproic acid-induced autism model rat. Neurosci Res 2010;66:2–6.

[15] Thompson WW, Price C, Goodson B, Shay DK, Benson P, Hinrichsen VL, et al. Early thimerosal exposure and neuropsychological outcomes at 7 to 10 years. N Engl J Med 2007;357:1281–92.

[16] Price CS, Thompson WW, Goodson B, Weintraub ES, Croen LA, Hinrichsen VL, et al. Prenatal and infant exposure to Thimerosal from vaccines and immunoglobulins and risk of autism. Pediatrics 2010;126:656–64.

[17] Strömland K, Nordin V, Miller M, Akerström B, Gillberg C. Autism in thalidomide embryopathy: a population study. Dev Med Child Neurol 1994;36:351–6.

[18] Williams G, King J, Cunningham M, Stephan M, Kerr B, Hersh JH. Fetal valproate syndrome and autism: additional evidence of an association. Dev Med Child Neurol 2001;43:202–6.

[19] Faro LR, Rodrigues KJ, Santana MB, Vidal L, Alfonso M, Durán R. Comparative effects of organic and inorganic mercury on in vivo dopamine release in freely moving rats. Braz J Med Biol Res 2007;40:1361–5.

[20] Ye W, Shimamura K, Rubenstein JLR, Hynes MA, Rosenthal A. FGF and Shh signals control dopaminergic and serotonergic cell fate in anterior neural plate. Cell 1998;93:755–66.